

Underwater image quality enhancement through Rayleigh-stretching and averaging image planes

Ahmad Shahrizan Abdul Ghani^{1,2} and Nor Ashidi Mat Isa¹

¹*Imaging and Intelligent System Research Team (ISRT), School of Electrical & Electronics Engineering, Engineering Campus, Universiti Sains Malaysia, 14300 Nibong Tebal, Penang, Malaysia*

²*Faculty of Electrical & Automation Engineering Technology, TATI University College, Jalan Panchor, 24100 Kijal, Kemaman, Malaysia*

ABSTRACT: *Visibility in underwater images is usually poor because of the attenuation of light in the water that causes low contrast and color variation. In this paper, a new approach for underwater image quality improvement is presented. The proposed method aims to improve underwater image contrast, increase image details, and reduce noise by applying a new method of using contrast stretching to produce two different images with different contrasts. The proposed method integrates the modification of the image histogram in two main color models, RGB and HSV. The histograms of the color channel in the RGB color model are modified and remapped to follow the Rayleigh distribution within certain ranges. The image is then converted to the HSV color model, and the S and V components are modified within a certain limit. Qualitative and quantitative analyses indicate that the proposed method outperforms other state-of-the-art methods in terms of contrast, details, and noise reduction. The image color also shows much improvement.*

KEY WORDS: Underwater image processing; Histogram modification; Contrast enhancement; Noise reduction.

INTRODUCTION

Underwater image processing is a challenging field that has received considerable attention because of the physical properties involved in such an environment. The importance of underwater activities in discovering and recognizing underwater imaging has resulted in new challenges and raised significant problems because of light absorption and diffusion effects (Gasparini and Schettini, 2003; Church and White, 2003; Shamsudin et al., 2012). Captured images tend to become greenish or bluish as they go deeper into the ocean. However, analytical techniques and methods to improve the quality of underwater images are still limited.

Underwater image normally has several problems, including limited range of visibility, low contrast, non-uniform lighting, bright artifacts, noise, blurring, and diminishing color (Shamsudin et al., 2012). As light travels in water, a rapid exponential loss of light intensity occurs depending on the color spectrum wavelength. According to Legris et al. (2003), light attenuation limits the visibility distance at about 20 m in clear water and 5 m or less in turbid water. In clear open waters, visible light is absorbed at the longest wavelengths first (Schettini and Corchs, 2012). Red, the most affected color, is reduced to one-third of its intensity after 1 m and is essentially lost after a distance of 4 m to 5 m underwater (Hitam et al., 2013). Compared with other wavelengths, blue and violet lights are absorbed last. Therefore, open ocean water appears deep blue to the human eye.

Corresponding author: *Ashidi Mat Isa*, e-mail: *ashidi@usm.my*

This is an Open-Access article distributed under the terms of the Creative Commons Attribution Non-Commercial License (<http://creativecommons.org/licenses/by-nc/3.0>) which permits unrestricted non-commercial use, distribution, and reproduction in any medium, provided the original work is properly cited.

Fig. 1 shows a visual illustration of diminishing underwater color. The figure shows that at the depth of 5 m, the red color is first absorbed by water. Absorption is then followed by orange, yellow, green, and blue (Hitam et al., 2013). Normally, underwater images appear green-blue because these color components are the last to be absorbed.

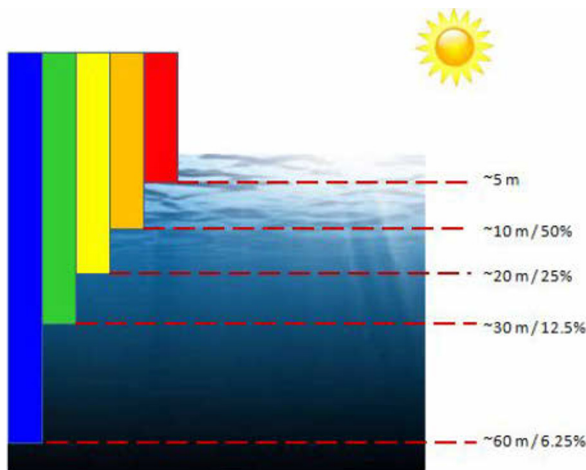


Fig. 1 Illustration of diminishing under water color (Hitam et al., 2013).

Color absorption causes captured underwater images to have low color and contrast performance. Important information from the image is also lost. Therefore, to restore the contrast, color, and loss information from images, the application of computer vision and image processing is necessary.

Contrast enhancement techniques are commonly used on underwater images to improve contrast performance and achieve a high dynamic range. The development of contrast enhancement techniques has attracted considerable attention in recent years, although it still remains an immature area compared with that of the normal image.

In this paper, a new method for image quality enhancement for underwater images is proposed. In terms of quality enhancement, this paper aims to improve image details and noise reduction, aside from improving underwater image contrast. The rest of the paper is organized as follows: Section 2 describes the existing techniques proposed by previous researchers. Section 3 explains the proposed technique in detail. Section 4 discusses the performance analysis and data samples. Qualitative and quantitative results are presented in Section 5. Section 6 presents the conclusion.

LITERATURE REVIEW

Underwater image processing can be addressed from two points of view: an image restoration technique and an image enhancement method (Schettini and Corchs, 2012). Image restoration focuses on recovering a degraded image using a model of the degradation of the original image formation. This method is rigorous and requires a number of model parameters, such as attenuation and diffusion coefficients, which characterize water turbidity (Schettini and Corchs, 2012). Alternatively, the image enhancement method uses qualitative and subjective criteria to produce a more visually pleasing image without depending on any physical model for image formation. The methods proposed by previous researchers mostly involve the modification of the values of image pixels that contribute to the changes in image contrast and colors.

Trucco and Olmos-Antillon (2006) devised a self-tuning image restoration filter that simplifies the well-known underwater image formation model of Jaffe (1990) and McGlamery (1979). This model proposes that an underwater image can be represented as a linear superposition of three components: direct component (light reflected directly by the object that has not been scattered in the water), forward-scattered component (light reflected by the object that has been scattered at a small angle), and back-scattered component (light reflected by the objects not on the target scene but by that enters the camera because of other reasons, such as floating particles). Rizzi et al. (2003) proposed unsupervised digital image color equalization with simultaneous global and local effects. Schechner and Karpel (2004; 2005) analyzed the physical effects of visibility degradation and proposed an image recovery algorithm based on several images taken through a polarizer at different orientations. However, the disadvantages of physics-based methods are that they require high computing resources and consume long execution time.

Naim and Isa (2012) proposed a method called Pixel Distribution Shifting Color Correction (PDSCC) for digital color image to correct the white reference point and ensure that the white reference point is achromatic. From the viewer side, the method corrects the image color to become more natural. The method also intervenes with the saturation problem of the image. However, it does not significantly increase the image contrast.

Iqbal et al. (2007) proposed the Integrated Color Model (ICM) and the unsupervised color correction method (UCM) (Iqbal et al., 2010). In Iqbal et al. (2007), the output image in the RGB color model is stretched over the entire dynamic range. The image is then converted to the HSI color model. In this color model, the S and I components are applied with contrast stretching. After stretching, the image in HSI color model is then converted back into the RGB color model to produce an enhanced output image. Iqbal et al. (2010) modified two color channels, red and green, based on the Von Kreis hypothesis to reduce the color cast. Contrast correction is then applied in the RGB color model. The image histograms are stretched at one or both sides based on the minimum and maximum values of each channel taken at 0.2% and 99.8% at the minimum and maximum points of the original histogram, respectively. Contrast stretching toward the upper side is applied to red, which is the lowest intensity channel. Contrast stretching at both sides is applied to green, which is the middle intensity value of the color channels, and contrast stretching at the lower side is applied to blue, which is the dominant color cast (Iqbal et al., 2010). For underwater images, the image is further converted into the HSI color model, and the S and I components are stretched at both the lower and upper sides. The overall contrast performances of the output images for both techniques increase. Nevertheless, not much difference can be observed in the output images using both techniques.

Overall observations indicate that in some areas, the images become under-enhanced where the areas become darker. The main drawback of the techniques reviewed above is that they produce noise.

METHODOLOGY: RAYLEIGH-STRETCHING AND AVERAGING OF IMAGE PLANES

This paper aims to extend the ICM (Iqbal et al., 2007) and the UCM (Iqbal et al., 2010) proposed by Iqbal et al. for underwater image by increasing contrast, reducing noise, and increasing the details in underwater image. ICM is a contrast correction technique based on histogram modification in RGB and HSI color models. The histograms of the original image are stretched over the entire dynamic range of the output gray level. UCM applies histogram stretching taken at 0.2% from the minimum and maximum gray-level values of the original histogram. Therefore, the histograms of the original image are taken from 0.2% to 99.8% and stretched into the entire range of the output gray level. The histogram is stretched on one or both sides based on the corresponding color channel. The image is then converted into the HSI color model, in which the S and I components are stretched for both lower and upper sides.

In this paper, the idea of histogram stretching is applied but in a manner different from that used in the ICM and the UCM. Fig. 2 shows the process of the proposed method. The proposed method is a modification of the ICM (Iqbal et al., 2007) and the UCM (Iqbal et al., 2010) proposed by Iqbal et al. The ICM and the UCM show an improvement in terms of contrast but produce high noise in the output image. The image detail does not significantly increase as some areas are under- and over-saturated. Therefore, the proposed method focuses on improving image contrast, reducing noise, and increasing image details. These parameters are evaluated using Peak Signal to Noise Ratio (PSNR) (Hitam et al., 2013), Mean Square Error (MSE) (Hitam et al., 2013), and entropy (Wu et al., 2005).

Underwater image usually consists of bright and dark areas. Overall image contrast can be increased by the global stretching of the image. The contrast of the image needs to be increased to increase the brightness of darker areas. However, global stretching also leads to an increase in the brightness of the bright areas, leading to the over-enhancement of the bright areas. These over-enhanced areas cause image pixels to become too bright, resulting in loss of details. The same problem occurs when global stretching is applied to the darker areas because it produces under-enhanced areas that reduce image details.

The proposed method, which uses two different image contrasts, addresses these issues. The idea of the proposed method is to produce two images with different contrasts: one as an under-enhanced image and another as an over-enhanced image. These two images are produced from a single image. The following steps briefly explain the method of producing two images from a single channel in the RGB color model. These steps are applied for other channels.

The mid-point of the original histogram is determined to produce the under- and over-enhanced images. The histogram is then divided into two regions and stretched based on this mid-point. The stretching process is applied to the images with respect to the Rayleigh distribution (Hitam et al., 2013; Eustice et al., 2002). This process produces two images with different contrasts.

The two produced images are stacked together, and the average value between the two images is calculated. The image is then converted into the Hue-Saturation-Value (HSV) color model. The S and V components of the HSV color model are stretched within the dynamic range of 1% from the minimum to the maximum values. The final image is obtained by converting the image back into the RGB color model.

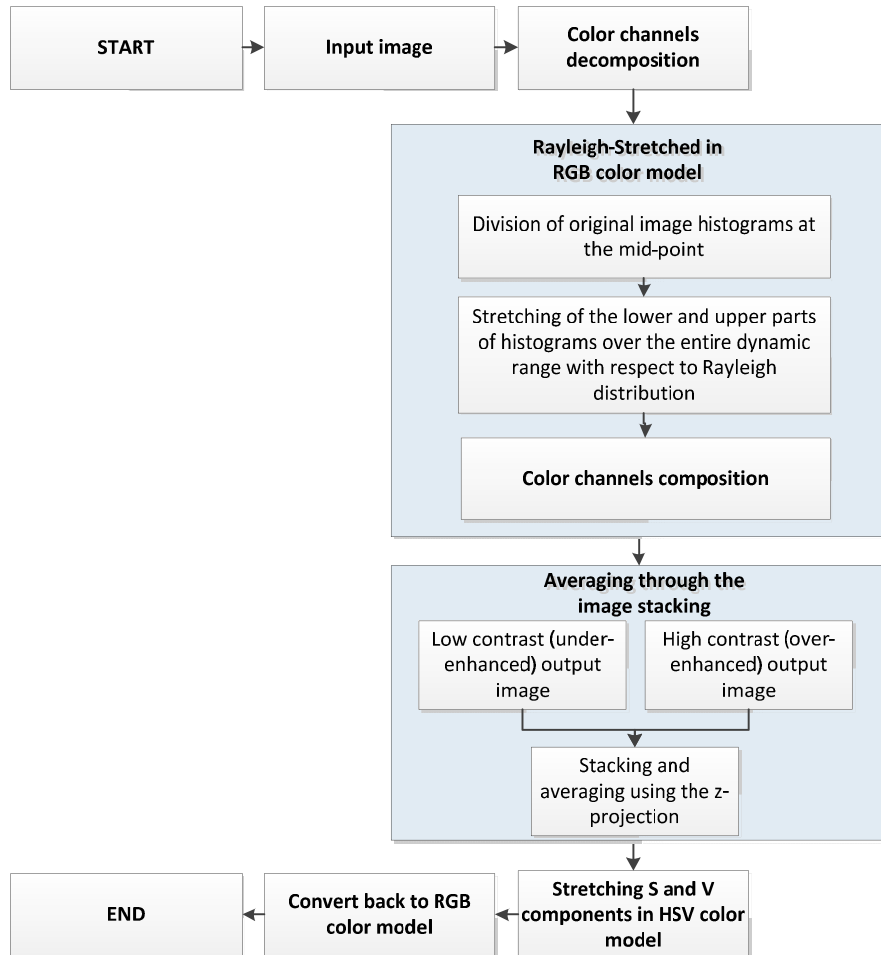


Fig. 2 Overall process of the proposed method.

Histogram stretching in the RGB color model with respect to the Rayleigh distribution

After the decomposition of image into its color channels in the RGB color model, the original histograms of the channel are divided at the mid-point of their intensity level. Eq. (1) is applied to calculate the mid-point of the intensity level, i_{mid} , of the original histogram. This equation is applied to all three channels of the RGB color model to determine the mid-point of the intensity level.

$$i_{mid} = \frac{I_{\max} - I_{\min}}{2} + I_{\min} \quad (1)$$

where I_{\max} and I_{\min} indicate the maximum and minimum intensity levels of the channel, respectively.

After calculating the mid-point, two regions of intensity levels are produced. The lower region consists of the value between the minimum intensity level and the mid-point of the original histogram, whereas the upper region consists of the value between the mid-point and the maximum intensity level value of the original histogram. These two regions are stretched over the entire dynamic range of the output intensity level.

Through histogram stretching, the image pixels are distributed over the dynamic range of the intensity level with respect to the Rayleigh distribution. The Rayleigh distribution refers to the bell-shaped distribution that concentrates most of the pixels to the middle of the intensity level. The upper and lower sides of the intensity level of the histogram have the lowest amount of pixels. The Rayleigh distribution is the best distribution for the histogram of underwater images (Hitam et al., 2003; Eustice et al., 2002).

The original equation of histogram stretching is given by Eq. (2) (Iqbal et al., 2010):

$$P_{out} = (P_{in} - i_{min}) \left(\frac{o_{max} - o_{min}}{i_{max} - i_{min}} \right) + o_{min} \quad (2)$$

where P_{in} and P_{out} are the input and output pixels, respectively, and i_{min} , i_{max} , o_{min} and o_{max} are the minimum and maximum intensity level values for the input and output images, respectively.

The probability distribution function of the Rayleigh distribution is given by Eq. (3):

$$PDF_{Rayleigh} = \left(\frac{x}{\alpha^2} \right) e^{\left(\frac{-x^2}{2\alpha^2} \right)} \text{ for } x \geq 0, \alpha > 0, \quad (3)$$

where α is the distribution parameter of the Rayleigh distribution and x is the input data, which is the intensity value in this case.

Eq. (2) is integrated into Eq. (3) to apply the Rayleigh-stretched distribution, thus producing the Rayleigh-stretched distribution as in Eq. (4).

$$Rayl.-stretched = \frac{\left[(P_{in} - i_{min}) \left(\frac{o_{max} - o_{min}}{i_{max} - i_{min}} \right) + o_{min} \right]}{\alpha^2} \cdot e^{\left[\frac{(P_{in} - i_{min}) \left(\frac{o_{max} - o_{min}}{i_{max} - i_{min}} \right) + o_{min}}{2\alpha^2} \right]^2} \quad (4)$$

The output histogram is stretched over the entire dynamic range so the values of o_{max} and o_{min} can be substituted with the values of 255 and 0, respectively. Therefore, Eq. (4) can be simplified as Eq. (5):

$$Rayl.-stretched = \frac{255(P_{in} - i_{min})}{\alpha^2(i_{max} - i_{min})} \cdot e^{\frac{-[255(P_{in} - i_{min})]^2}{2\sigma^2(i_{max} - i_{min})^2}} \quad (5)$$

where i_{min} and i_{max} indicate the minimum and maximum intensity level values for input image in each region, respectively. For the lower region, i_{min} indicates the minimum intensity level value in each channel, and i_{max} indicates the maximum intensity level value in the region, which is equivalent to the mid-point value of the original histogram. For the upper region, i_{min} indicates that the minimum intensity level value in the region is equivalent to the mid-point value of the histogram, and i_{max} indicates that the maximum intensity level value in the region is equivalent to the maximum intensity level of the original histogram. The described processes are applied to all channels of RGB color model.

Fig. 3 shows an example of the histogram with its maximum, minimum, and mid-points. The original histogram is divided at its mid-point to produce two separate histograms. These two histograms are stretched over the entire dynamic range of [0, 255] with respect to the Rayleigh distribution.

After applying these processes to the corresponding channels, all lower-stretched histograms are composed to produce an image and all upper-stretched histograms are also composed to produce another image. This process produces two different images with different contrasts. The lower region of the histogram produces an under-enhanced image, whereas the upper region produces an over-enhanced image. These two images are composed using the average values between these images. This process is explained in the next subsection.

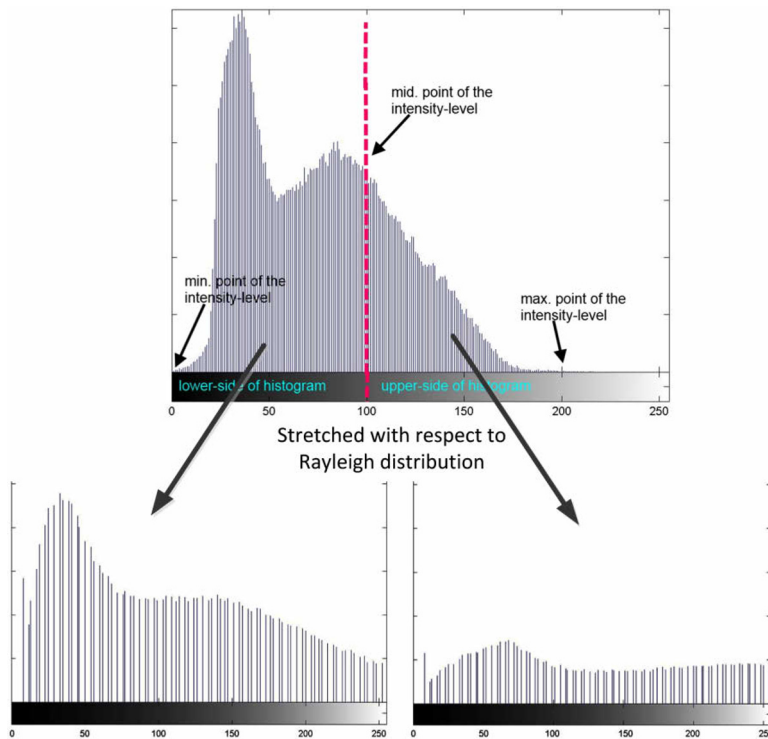


Fig. 3 Original histogram divided into two separate histograms at its mid-point.

Stacking and averaging using z-projection

The images are stacked together to obtain the average of the image pixels between these two images. With the z-axis as reference, the images are aligned together so that the images are located perpendicular to the z-axis and the image plane itself. The under-enhanced image is then projected with the over-enhanced image. Each pixel of both images is compared at a particular pixel location, and the average value from these pixels is determined.

This process produces an improved image in terms of contrast, with the output image having excellent contrast. Color performance is also improved. Fig. 4 shows a visual illustration of the combination and averaging of both under- and over-enhanced images. The resultant image has average values between the under- and over-enhanced images as well as excellent contrast and visibility.

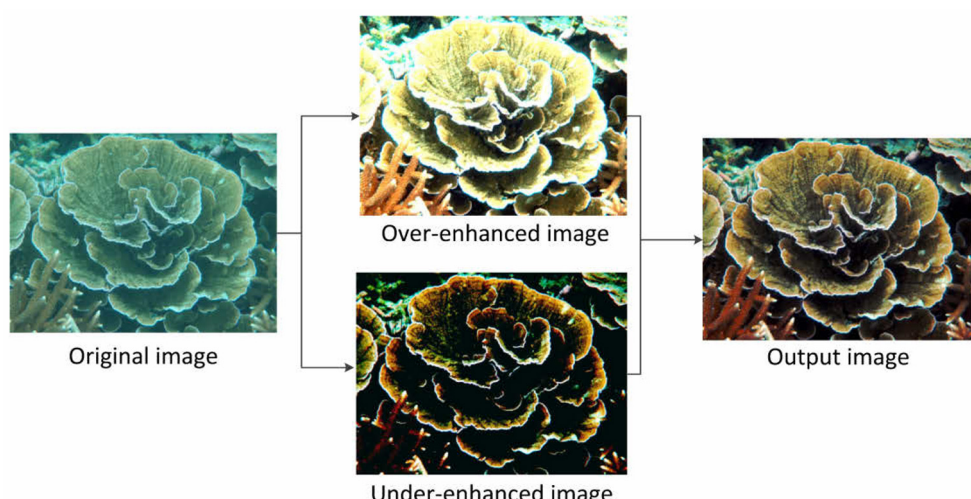


Fig. 4 Combination of the under- and over-enhanced images through stacking and averaging along the z-axis to produce the output image.

Stretching of the S and V components in the HSV color model

As a final step in the proposed method, the image is converted into the HSV color model (Hitam et al., 2013). The conversion method and details of this color model are clearly explained in (Hitam et al., 2013). This step is included in the proposed method to correct the saturation and brightness of the final image. The pixel distribution of the image in terms of saturation and brightness can be improved by stretching the S and V components because the pixels are distributed through the dynamic range of S and V. In addition to this process, a limit of 1% is applied to both components at the minimum and maximum values. Therefore, the stretching process is applied within the range of [1%, 99%]. This 1% limit is taken from the experiment conducted by (Shamsudin et al., 2012). The tested images tested with 1% limit at minimum and maximum values of the S and V components in this paper indicate excellent contrast performance. Appendix A shows the results.

These limits are necessary to avoid the image from become under- or over-saturated. Fig. 5 shows an illustration of the new ranges of the S and V components of the HSV color model applied in the proposed method.

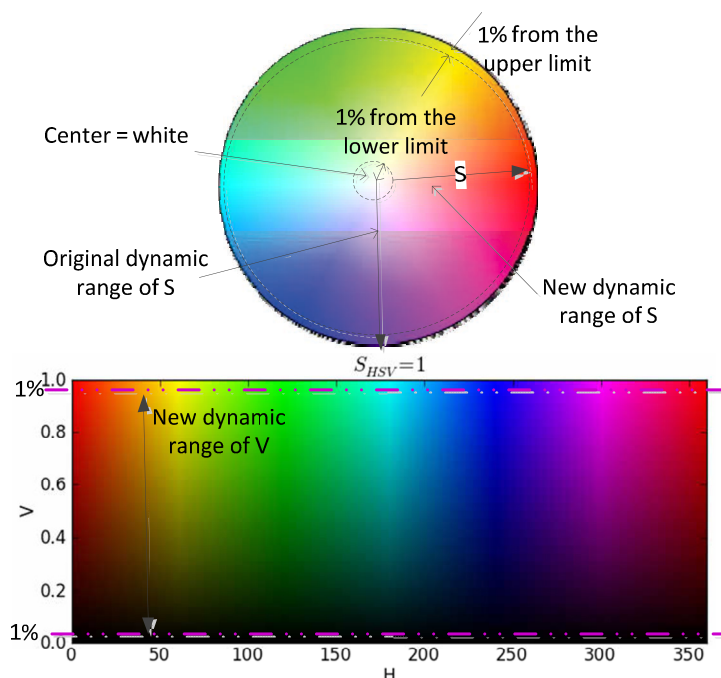


Fig. 5 New range of the S and V components of the HSV color model within the 1% limit from the maximum and minimum values.

PERFORMANCE ANALYSIS AND DATA SAMPLES

As previously mentioned, the proposed method aims to improve the methods of ICM and UCM which are proposed by Iqbal et al. (2007; 2010). Both ICM and UCM methods increase the underwater image contrast. However, there is a drawback of these methods as ICM and UCM produce high noise in the output images. In addition, the output image sometimes becomes darker and too bright resulting in under- and over-saturated.

These problems are addressed in the proposed method. The proposed method is designed to improve the quality of underwater image in terms of contrast, details, and noise reduction. Three quantitative parameters namely, entropy, MSE, and PSNR are used in the evaluation. Nevertheless, most of the previous researchers measure the improvement of image quality through visual inspection (Schettini et al., 2012). A few of them use quantitative estimation and residual error which are computed between ground truths and corrected images (Schettini et al., 2012). In this paper, the evaluation of image contrast is done through the visual inspection in section 5.1. On the other hand, the evaluation of image details could also be done partially through visual inspection in section 5.1. In addition to that, the image details are also evaluated through the value of entropy, which provides better and clear comparison between compared images. The values of MSE and PSNR are used to evaluate the image noise. The following subtopics will discuss in details the parameters used in this paper.

Image contrast

To evaluate the image contrast, the visual inspection of the image is done. In this paper, image contrast is evaluated through visual inspection in section 5.1. Contrast of an image is quantitatively hard to measure. Moreover, there are several more definitions proposed for contrast measurement as stated in Rizzi et al. (2004). However, there is no reference to compare between two images in terms of contrast. Contrast value is just a scale. Low value of contrast causes the image contrast to under-saturate whereas high value of contrast causes the image contrast to over-saturate. The optimal contrast should lie between low and high contrast values. However, there is no comparative contrast value to show that one image is better than the other image in terms of contrast.

Michelson defined the contrast or luminance in general form as in Eq. (6) (Rizzi et al., 2004; Michelson, 1927):

$$L(x, y) = L_0 [1 + Nf(x, y)] \quad (6)$$

where L_0 is the background luminance and N is defined as Nominal Contrast. $f(x, y)$ is limited to [-1;1]. In case that $f(x, y)$ is a sinusoid, the contrast, C_m is defined as in Eq. (7) (Rizzi et al., 2004; Michelson, 1927). L_{\max} and L_{\min} are maximum and minimum luminance of an image, respectively. It is however a global contrast measurement.

$$C_m = \frac{L_{\max} - L_{\min}}{L_{\max} + L_{\min}} \quad (7)$$

However, these quantitative measures of contrast are not suitable for natural image as consequence of its characteristics (Rizzi et al., 2004).

King-Smith and Kulikowski (1975) define the contrast, C_{kk} as in Eq. (8). L_{\max} and L_0 refer to maximum and background luminance, respectively.

$$C_{kk} = \frac{L_{\max} - L_0}{L_0} \quad (8)$$

Whittle (1986) defined the contrast, C_w as in Eq. (9). ΔL is equal to L_{\max} / L_{\min} .

$$C_w = \frac{\Delta L}{L_{\min}} \quad (9)$$

Reinagel and Zador (1999), proposed a model which considered of extracting N pixels corresponding to the areas upon which the human eye dwells during the process of vision of an image. In their experiment, only the white and black images are considered. The contrast, C is defined as Eq. (10).

$$C = \frac{\sum_k \left[\sum_{i,j} \left(I_{i,j} / I_k \right)^2 \right]^{1/2}}{I \prod_k} \quad (10)$$

where:

I_{ij} is the intensity of the pixels at coordinates (i, j)

I_k is the average intensity of the k -th patch

I is the average image intensity

\prod_k area of 23×23 pixels (approximating 1°) around the pixels N

As there are various definitions of image contrast, it is the best way to allow the observers to evaluate the contrast from their own Human Visual System (HVS). Contrast of an image is defined as the image characteristic or view that is pleasant to the human visual system. Therefore, in the proposed method of Rayleigh-Stretching and Averaging Image Planes, the evaluation of image contrast is done through the visual observation in qualitative result in section 5.1. ICM and UCM produce sometimes excessive contrast. Figs. 6(b) and 6(c) show the output images produced by ICM and UCM. Both of the output images seem identical to each other. The blue coral in the image is too bright resulting in excessive blue-green illumination. This causes the image contrast to become over-saturated. Moreover, the border of blue coral could not be seen clearly in the image. This problem is addressed in the proposed method.

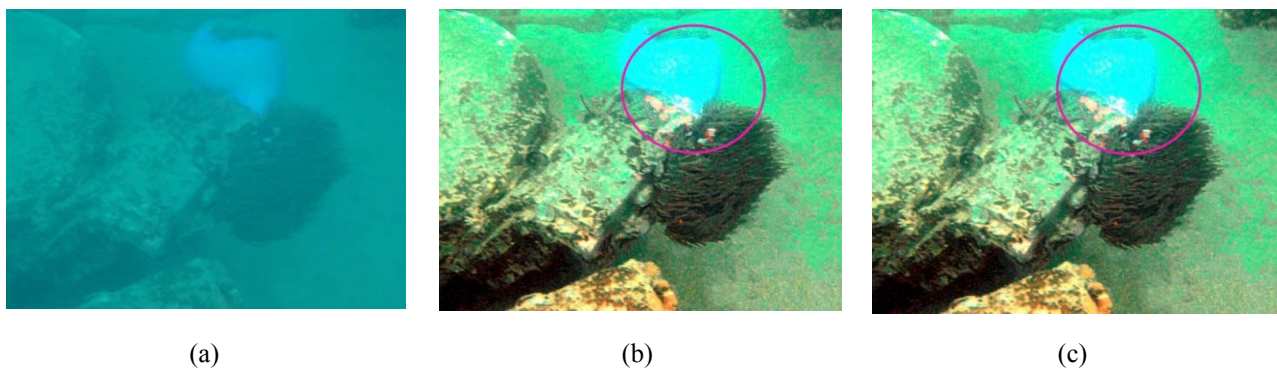


Fig. 6 Blue coral. (a) Original image, (b) image processed using ICM method, and (c) image processed using UCM method.

Further contrast enhancement of underwater images using the proposed method is discussed in section 5.1 and in Appendix A.

Mean squared error (MSE) and peak signal to noise ratio (PSNR)

Noise is defined as the random fluctuations in the signal intensity. It is produced from the interfering signals from electronics system of the captor device. Noise is assumed as uncorrelated with respect to the image, which means that there is no relationship between the pixels and noise values. Usually, the shape of noise model will takes place on each of the uncorrupted pixel values. Therefore, to restore the original signal, the unwanted pixel values that shape the noise should be removed.

MSE and PSNR are the quantitative metrics used to compare the improved image and original image. These quantitative metrics are used and mentioned by researchers in Schettini and Corchs (2012), Hitam et al. (2013), Kumar and Rattan (2012). MSE and PSNR are widely used to measure the degree of image distortion because they can represent the overall gray-value error contained in the entire image and mathematically tractable as well. With MSE or PSNR, only gray-value differences between corresponding pixels of the original and the distorted version are considered. In terms of quality assessment and distortion metrics, PSNR and MSE are the most widely used Schettini and Corchs (2012). Therefore, based on the standard quantitative measurement, the proposed method uses MSE and PSNR as they are the most quality assessment metrics used by previous researchers and widely used in the image evaluation.

MSE is used as signal fidelity measure. The main function of signal fidelity measurement is to compare two signals by providing a quantitative score to determine the level of error or distortion between them (Ndajah et al., 2011). MSE is computed by averaging the squared intensity differences of distorted and reference image pixels. MSE is given by the Eq. (11). $I_1(m, n)$ and $I_2(m, n)$ represent the intensity value of the original (reference) and improved images, respectively. Depending on the image format, the intensity value of an image could be in double or unsigned integer which is normally used by previous researchers. In the proposed method, the image used is in the format of unsigned integer 8, means that the image has 256 gray-level. $M \times N$ denotes the size of the image, and m and n indicate the x and y locations of the pixels of the image. The lower the value of MSE, the lower the error or noise is.

$$MSE = \frac{1}{M \times N} \sum_{m,n} [I_1(m,n) - I_2(m,n)]^2 \quad (11)$$

Nevertheless, MSE is usually expressed as the PSNR. PSNR indicates the ratio of the maximum possible signal and the noise that affect the image representation. The term $(2^8 - 1)$ refers to the maximum possible signal of the image. As unsigned integer 8 image is used, the maximum possible signal will become $(2^8 - 1)$ which is equal to 255. 255 is the highest intensity value for the image in unsigned integer 8 format. High value of PSNR indicates the high quality of image. PSNR is defined by the MSE. It is given by the Eq. (12) (Hitam et al., 2013; Kaushik and Sharma, 2012):

$$PSNR = 10 \log_{10} \frac{(2^B - 1)^2}{\sqrt{MSE}} = 20 \log_{10} \frac{(2^B - 1)}{\sqrt{MSE}}, \quad (12)$$

where B represents the bits per sample. In this paper, $B = 8$ as the unsigned integer 8 image is used. The best resultant image is indicated by low MSE and high PSNR.

Image details/information (Entropy)

Entropy or discrete entropy is used as quality assessment in Wu et al. (2005), Wu and Li (2013), Ye (2009), Padmavathi et al. (2010) and Singhai and Rawat (2007). Entropy represents the abundance of image information. Entropy is a measure of image information content, which is interpreted as the average uncertainty of information source (Ye, 2009). In an image, entropy is defined as corresponding states of intensity-level which individual pixels can adopt. The entropy in an 8 bit image with 256 gray-level is maximum if all gray-level are occupied and have equal probability distribution function. Information content, I_i of a particular intensity-level is defined as Eq. (13), where $p(x)$ is the probability distribution function of a certain gray-level.

$$I_i = -\log_2 p(x) \quad (13)$$

Entropy is calculated as the summation of the products of the probability of outcome multiplied by the log of the inverse of the outcome probability. As stated in Wu et al. (2005) and Ye (2009), the entropy in Eq. (14) is used to measure the image information. The performance of image details or image information in the proposed method is also measured using this formula.

$$H(X) = -\sum_{x=1}^k p(x) \log_2 p(x) = -\text{sum}(p \cdot \log_2(p)) \quad (14)$$

$p(x)$ is equal to p which represents the probability distribution function of the image at the state x (pixel). k is the total number of intensity-level. If an image is in the format of unsigned integer 8, it will be $[11111111_b]$ in binary number (8 bit), then there will be 256_d (decimal) intensity-level which means that the first intensity-level is 0 and the last intensity-level is 255. In this paper, the images used are in the format of unsigned integer 8 which means that the first intensity-level ($x=1$) is 0 and the last intensity-level ($k=256$) is 255.

The image entropy can reflect the gray-scale information at location of the image pixel and the integrated characteristics of distribution within the pixel neighborhood under the premise of containing image information. Image entropy selects the neighborhood gray-scale average as a gray-scale image distribution characteristic of space which leads that blurry photos have smaller entropy values than the high-resolution ones. Moreover, in the process of restoration, with the changes of parameter values, the brightness of photos changes too. Most evaluation functions are affected by the brightness of photos. However image entropy relates to not only the distribution of image pixels but also the neighborhood gray-scale averages and when the brightness of photos changes, the image entropy will change little. If an image is clear with low brightness, other evaluation function may get small function value. However, image entropy considers the overall distribution of the image pixels, so its value will be large.

On the other hand, image details or image information could evaluate partly through the visual inspection of the image. Consider the image of blue coral in Fig. 6. By applying the ICM and UCM on the underwater image, the contrast and color of blue coral become over-saturated. The blue-green illumination of blue coral becomes almost identical to the background color. Therefore, the exact shape of blue coral becomes unknown and hardly differentiated from the background. This point is also addressed in the proposed method. The proposed method is designed to enhance the image contrast and produce a better output image which could differentiate between the objects and the background.

As previously mentioned, entropy represents the abundance of image information or image details. The higher entropy shows that the image has more information whereas low entropy indicates that the image has less information. The images produced by the proposed method have higher entropy values compared to the other methods. This shows that the images produced by the proposed method have more information and more details. To quantitatively evaluate the image details, the entropy value is used as it can provide better comparison of the image details.

Fig. 7 shows an example of underwater image, jellyfish. The image produced by HE becomes darker, reddish and some areas are over-saturated. The darker and over-saturated areas cause the image could not be seen clearly, thus reducing the image details. On the other hand, Jellyfish in the images produced by ICM and UCM become darker compared to original image and the sand contrast at the bottom of the image becomes over-saturated, resulting in the sand to become out of shape. However, the effect of over-contrast is observed more in the image produced by UCM, where the sand becomes too bright and the shape of the sand could not be seen clearly. Therefore, UCM has less detail compare to ICM. Moreover, the jellyfish in the image produced by PDSCC is hardly differentiated with the background as it has the lowest contrast. Thus, the image detail is less compared to the other methods. On the other hand, the image produced by the proposed method is not too bright and not too dark. Thus, the jellyfish could be better seen and differentiated from the background. In addition, the shape of the sand is clearly seen in the image. Thus, the proposed method has more information.

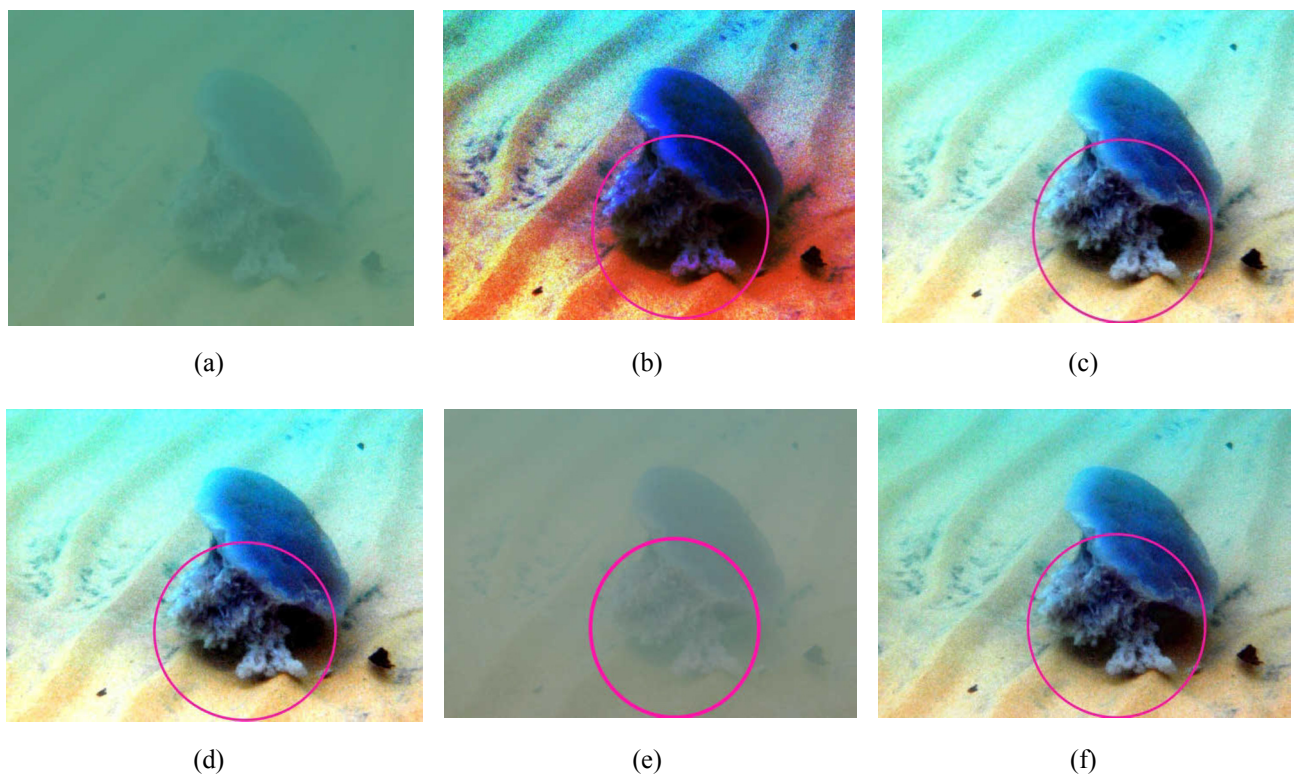


Fig. 7 Jellyfish: (a) original image. The rest are images processed using the following methods
 (b) HE, (c) ICM, (d) UCM, (e) PDSCC, (f) Proposed method

In addition to ICM and UCM, the evaluation of the underwater image is also compared with the other method namely Histogram Equalization (HE) and PDSCC. The next section will discuss about the methods of HE and PDSCC.

Histogram equalization (HE)

HE is chosen because it is the most commonly used by previous researchers and is the basic technique in histogram modification. HE is one of the most widely used methods in image enhancement because of its strong performance on almost all types of images. In general, HE solves some of the problems of surface images. HE works by flattening the histogram and stretching the dynamic range of the gray-levels by using the cumulative distribution function (PDF) and Cumulative Density Function (CDF). PDF of an image with intensity i is defined as the number of pixels with intensity i , n_i divided by the total number of image pixels, n as in Eq. (15) (Yeganeh et al., 2008; Senthilkumaran and Thimmiaraja, 2014). This will produce a scale of probability of occurrence of an intensity level in an image with normalized to 1.

$$PDF(i) = \frac{n_i}{n} \quad (0 \leq i \leq L) \quad (15)$$

L is total number of intensity level. On the other hand, the CDF is defined as the summation of the PDF with the total of 1 as in Eq. (16). The CDF is the Look-Up Table (LUT) for histogram equalization. To obtain the real value of intensity level, the CDF will be multiplied with the number of intensity level. In this case, it will be multiplied with 255 as the image is in format of unsigned integer 8. The original intensity value will be mapped to the new intensity level through this LUT.

$$CDF(i) = \sum_{i=0}^{L-1} PDF(i) \quad (16)$$

Applying HE to the image resulting in under- and over-contrast. As the image histogram stretched and flattened, low intensity values will become lower and high intensity values will become higher. These lower and higher intensity values cause the output image to produce under- and over-saturated areas. In addition, for RGB image, HE attempts to equalize the intensity percentage of three color channel, red, green, and blue. Underwater image normally has low red channel percentage. By applying HE to underwater image, red color channel percentage will have almost identical color percentage with green and blue. Excessive red color channel percentage cause the underwater image to become reddish.

More information about the HE could be found in Singhai and Rawat (2007), Yeganeh et al. (2008), Senthilkumaran and Thimmiaraja (2014) and Arici et al. (2009).

Pixel distribution shifting color correction (PDSCC)

PDSCC is the latest contrast enhancement technique that is also designed for underwater images. PDSCC employs a shifting process on the pixel distribution of a color image to correct its white reference point and ensure the white reference point is achromatic (Naim and Isa, 2012).

PDSCC extends the method of 3D rotational matrix (3DMAT) by implementing the modification on 2D two-color channel plane. 3DMAT is the first 3D rotational method used due to its simplicity of usage and fast execution. 3DMAT employs the 3D pixel distribution rotational by rotating the pixels three times (yaw, pitch, and roll) using three different rotational angles.

In the PDSCC, two 3D rotational methods for color correction are specifically designed to shift the pixel distribution of an image such that the surrounding insignificant illumination will be suppressed or removed from the output image. This is done by moving the pixel distribution of the image to the diagonal plane of 3D RGB color model. The shifting process is implemented on 2D two-color channel plane instead of on 3D RGB color model directly. These 2D color planes are constructed from 3D RGB color model, namely red-green plane, red-blue-plane, and green-blue plane (Naim and Isa, 2012). This process could ensure the surrounding illumination pixel distribution to be rendered achromatic.

RESULTS AND DISCUSSION

Underwater images are captured in three different Malaysian islands, namely, Tioman, Langkawi, and Perhentian, to evaluate the proposed method. Different images with different environments, objects, and backgrounds are tested and evaluated using the proposed method. As the method aims to improve the ICM (Iqbal et al., 2007) and UCM (Iqbal et al., 2010) in terms of details and noise, the proposed technique is compared with these two methods in terms of entropy, MSE, and PSNR.

Two other methods are also used for comparison, namely, the PDSCC (Naim and Isa, 2012) and HE methods. PDSCC is the latest contrast enhancement technique that is also designed for underwater images. The HE is chosen because it is the most commonly used by previous researchers and is the basic technique in histogram modification.

Qualitative results

Three hundred underwater images were tested to evaluate the proposed method. These underwater images have very low contrast and visibility. The objects in the images are unclear, making differentiate between the objects and the background difficult. In addition to the image of jellyfish in Fig. 7, three more underwater images are shown in this paper as examples. Figs. 8 to 10 show examples of images processed using the proposed method in comparison with the other methods. The circled areas in each image show the clear differences between these compared images.

The image of blue coral in Fig. 8 shows that the image produced by HE is over-saturated as the image turns reddish. Moreover, the contrast of blue coral becomes over-saturated. The same problem occurs when ICM and UCM are used, as the blue coral become over-saturated and excessive blue illumination is seen. When the PDSCC is used, the output image worsens because, although the blue illumination is partially removed, the object color becomes unnatural. Conversely, in the image produced by the proposed method, the contrast increases to a level in which the image is not saturated or over-enhanced. The circled areas in the figures clearly show the differences.

The output image of the HE for the red fish in Fig. 9 shows that the image becomes reddish and over-saturated. The images produced by ICM and UCM are also over-saturated as the images retain more blue-green illumination and the sand is out of shape. On the other hand, the image produced by the PDSCC has some blue-green illumination removed, but the contrast is not significantly improved because the fish cannot be differentiated clearly from the background and the sand remains out of shape. Image produced by the proposed method does not produce over-saturated contrast, as the shape of sand is clearly seen.

The circled area in Fig. 10 shows that the image produced by the HE is over-saturated as the image becomes too bright, resulting in the reduction of the image details. The images produced by the ICM and UCM indicate an improvement in terms of contrast. However, the output images become darker than those of the proposed method. A darker image causes loss of details in several areas. The PDSCC improves only a small amount of contrast as the blue-green illumination of the water remains in the output image.

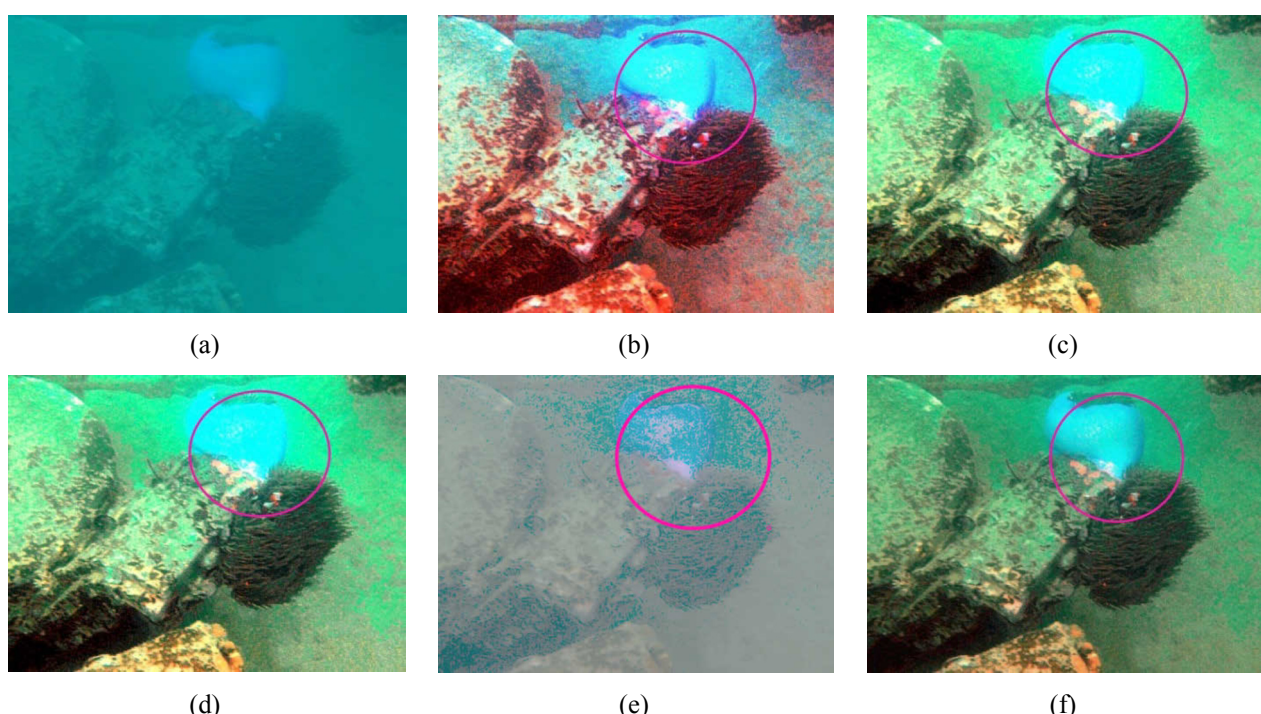


Fig. 8 Blue coral: (a) original image. The rest are images processed using the following methods
(b) HE, (c) ICM, (d) UCM, (e) PDSCC, (f) Proposed method

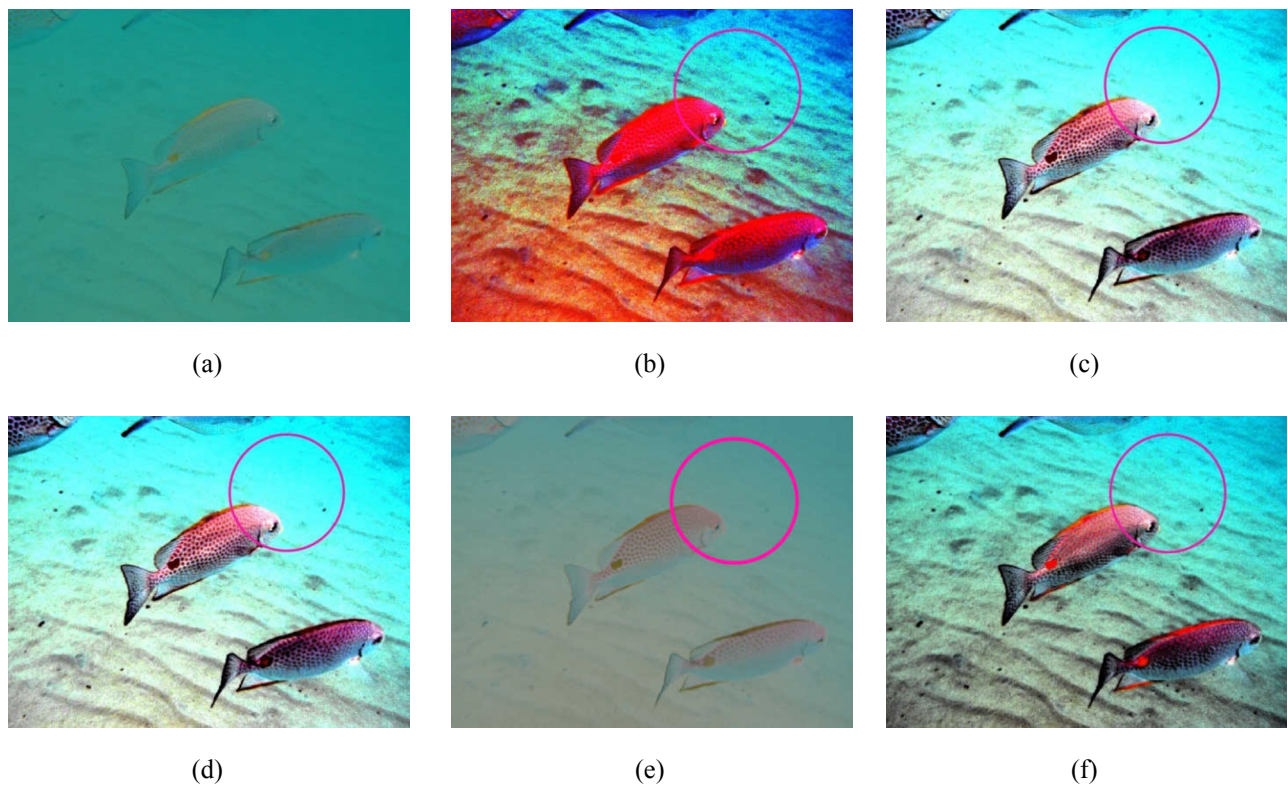


Fig.9 Red fish: (a) original image. The rest are images processed using the following methods
(b) HE, (c) ICM, (d) UCM, (e) PDSCC, (f) Proposed method

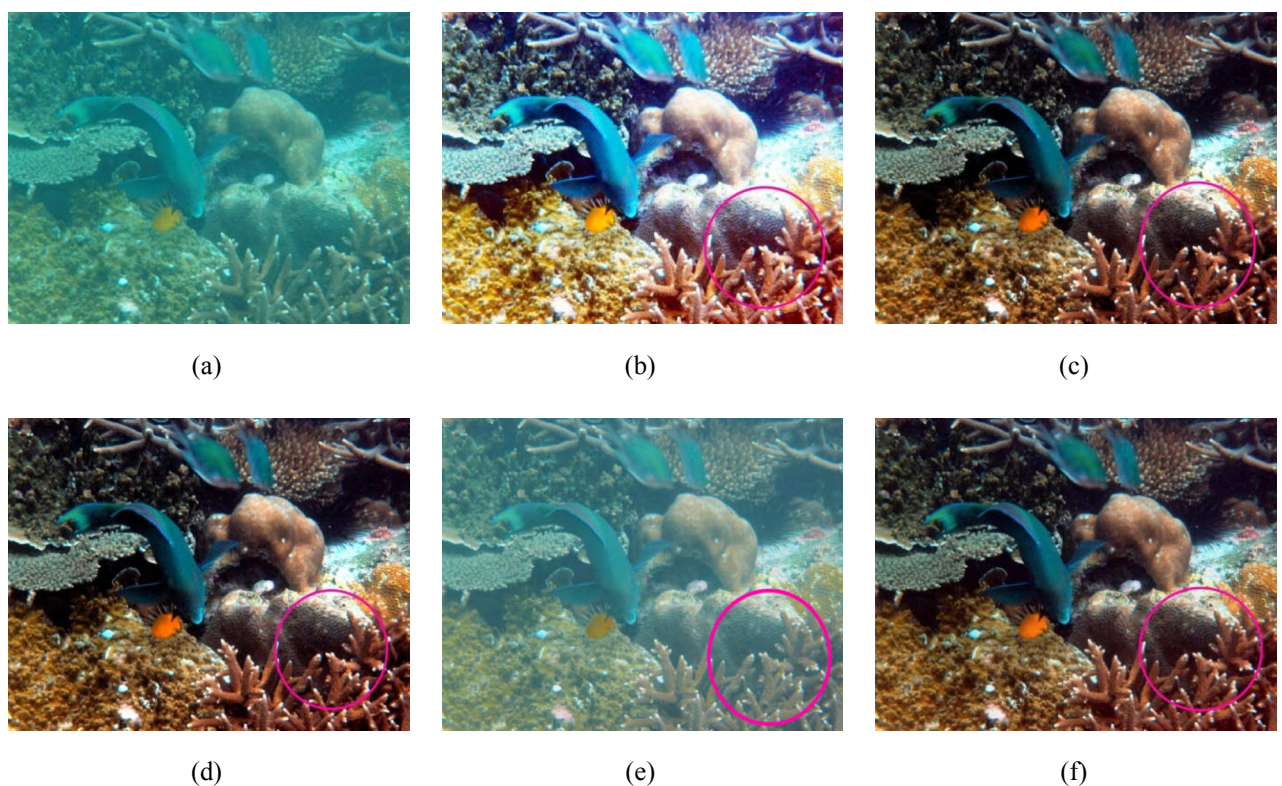


Fig. 10 Blue fish: (a) original image. The rest are images processed using the following methods
(b) HE, (c) ICM, (d) UCM, (e) PDSCC, (f) Proposed method

Overall visual observation indicates a significant improvement in the contrast performance of the resultant images by the proposed method unlike in other methods. Contrast and color performances of the objects also improve, and the objects are better differentiated from the background. These criteria from visual observations prove that the proposed method improves image contrast better than other methods.

Appendix A shows more qualitative results of the tested underwater images. In Appendix B, the quantitative evaluation of the images in Appendix A is presented in a table. The best way to see the differences is by zooming in the image. However, the differences of some images are hardly seen especially if the comparison is focused on image noise. In this case, the value of MSE and PSNR are used as comparison, which are normally used by previous researchers (Hitam et al., 2013). In Appendix A, the rectangular areas show the clear differences between the compared images. In the rectangular areas, the differences of the respective method can be seen whether the areas are over-saturated, darker (under-saturated), or has more blue-green illumination. Overall results in Appendices A and B show that the proposed method produced better images in terms of contrast, details, and noise reduction. HE over-saturates the image contrast as the images become reddish and darker. ICM and UCM improve the images contrast. However, at some point, the output images become darker and some areas become over-saturated resulting in loss of image details. Even PDSCC has lower MSE and higher PSNR, it improves only a small amount of contrast as the output image is hardly differentiated with the background. This is clearly verified and proven in section 5.1 and in Appendix A.

Quantitative result

As mentioned previously, the proposed method aims to improve the ICM and UCM methods proposed by Iqbal et al. The output images produced by ICM and UCM produce high noise and low details. The proposed method is presented to improve the details and reduce the noise in underwater images. Therefore, entropy, MSE, and PSNR are used as quantitative evaluation parameters. The MSE and the PSNR are two error metrics used to compare the quality of resultant images. The MSE is the cumulative squared error between the resultant and original images. The PSNR indicates the ratio of the maximum possible signal and the noise.

Table 1 shows the comparative values of entropy, MSE, and PSNR for images shown in Figs. 7 to 10. The quantitative performance of the proposed method is clearly better than that of the other methods in terms of entropy. A comparison of the results of the HE, the ICM, the UCM, and the PDSCC indicates that the proposed method has the highest entropy and that the resultant images of the proposed method contain the most details and information. However, in terms of MSE and PSNR, the proposed method is only second to the PDSCC. The PDSCC produces the lowest MSE and the highest PSNR for the four images. However, visual observation in section 5.1 indicates that the PDSCC cannot improve the contrast significantly as the blue-green illumination of the water remains. The objects in the image processed by the PDSCC cannot be seen clearly because of the limited difference in the object and its background. The PDSCC has low entropy, causing the resultant images to contain less detail.

These values also show that the proposed method successfully reduces the noise and increases valuable information in the image unlike the ICM and the UCM. These qualitative and quantitative evaluations indicate that the proposed method improves the quality of the underwater image.

Appendix A shows 20 additional examples of underwater images. The quantitative evaluation of these images is presented in Appendix B.

The dataset in Table 2 shows the average values of entropy, MSE, and PSNR for 300 tested underwater images. The proposed method leads other methods in terms of entropy as it has the highest value of entropy. The proposed method ranks second in terms of the MSE and the PSNR after the PDSCC.

These values indicate a degree of improvement in terms of contrast and lowering of the noise in the resultant image produced using the proposed method. Visual inspection shows that objects in the image are better differentiated than those obtained using other methods.

Table 1 Quantitative results in terms of entropy, MSE, and PSNR for images in Figs. 7 to 10.

Image	Method	Entropy	MSE	PSNR
Jellyfish	HE	5.544	4 975	11.16
	ICM	7.086	15 436	6.25
	UCM	6.764	15 445	6.24
	PDSCC	5.469	425	21.84
	Proposed method	7.782	4 210	11.89
Blue coral	HE	5.449	9 768	8.23
	ICM	7.291	15 003	6.37
	UCM	6.979	15 009	6.37
	PDSCC	6.037	5 320	10.87
	Proposed method	7.739	4 210	11.89
Red fish	HE	5.525	7 039	9.66
	ICM	6.692	13 491	6.83
	UCM	6.813	13 507	6.82
	PDSCC	5.756	1 834	15.50
	Proposed method	7.765	3 486	12.71
Blue fish	HE	5.955	4 320	11.78
	ICM	7.564	13 660	6.78
	UCM	7.579	13 659	6.78
	PDSCC	7.117	625	19.99
	Proposed method	7.615	3 845	12.28

Note: The values in bold typeface represent the best results obtained in the comparison.

Table 2 Average values of entropy, MSE, and PSNR for 300 underwater images

Method	Entropy	MSE	PSNR
ICM	7.613	14 373	6.60
UCM	7.605	14 377	6.60
PDSCC	7.088	897	20.58
HE	5.917	4 678	11.80
Proposed method	7.703	2 616	14.23

Note: The values in bold typeface represent the best results obtained in the comparison.

CONCLUSION

The proposed method successfully improves the contrast and reduces the noise of the original method of the ICM and the UCM previously proposed by Iqbal et al. The combination of the histogram modification in the RGB and the HSV color spaces increases the contrast of underwater image. The improvement of image color results in the increase in the visibility of the objects and better object recognition in the image. This method is expected to help further underwater research.

The overall results of the HE indicate that the image is over-saturated and become reddish, and thus image details are reduced. Even the resultant images produced by the PDSCC displays excellent MSE and PSNR. The image contrast does not significantly increase because the blue-green illumination is retained in the images. Several images are only partially increased, and only a part of water illumination is removed as shown in Fig. 8. Moreover, the objects and the background cannot be clearly seen and are hardly differentiated. No improvement in the image color is also observed.

ACKNOWLEDGMENT

The authors would like to thank the anonymous reviewers for their valuable comments and suggestions that helped significantly improve this paper. Special thanks to TATI University College for the education sponsorship grant. This work was partially supported by the Fundamental Research Grant Schema (FRGS) of the Ministry of Higher Education of Malaysia (MOHE) called “The Investigation of New Color Image Illumination Estimation Concept for the Development of New Color-Correction Techniques.”

REFERENCES

- Arici, T., Dikbas, S. and Altunbasak, Y., 2009. A histogram modification framework and its application for image contrast enhancement. *IEEE Transactions on Image Processing*, 18(9), pp.1921-1935.
- Church, S.C. and White, E.M., 2003. Ultraviolet dermal reflection and mate choice in the guppy. *Elsevier Sciences Ltd*, 65(4), pp.693-700.
- Eustice, R., Pizarro, O., Singh, H. and Howland, J., 2002. Underwater image toolbox for optical image processing and mosaicking in MATLAB. *Proceedings International Symposium on Underwater Technology*, Tokyo, 19 April 2002, pp. 141-145.
- Gasparini, F. and Schettini, R., 2003. Color correction for digital photographs. *12th International Conference on Image Analysis and Processing (ICIAP 2003)*, Mantova, 17-19 September 2003, pp.646-651.
- Hitam, M.S., Yussof, W.N.J.W. and Awalludin, E.A., 2013. Mixture contrast limited adaptive histogram equalization for underwater image enhancement. *IEEE International Conference on Computer Applications Technology (ICCAT)*, Sousse, 20-22 January 2013, pp.1-5.
- Iqbal, K., Odetayo, M., James, A., Salam, R.A. and Talib, A.Z., 2010. Enhancing the low quality images using unsupervised color correction method. *International Conference on System Man and Cybernetics (SMC)*, Istanbul, 10-13 October 2010, pp.1703-1709.
- Iqbal, K., Salam, R.A., Osman, A. and Talib, A.Z., 2007. Underwater image enhancement using integrated color model. *IAENG International Journal of Computer Science*, 34(2), pp.529-534.
- Jaffe, J.S., 1990. Computer modeling and the design of optimal underwater imaging systems. *IEEE Journal of Oceanic Engineering*, 15(2), pp.101-111.
- Kaushik, P. and Sharma, Y., 2012. Comaprison of different image enhancement technique based upon PSNR and MSE. *International Journal of Applied Engineering Research*, 7(11), pp.2010-2014.
- King-Smith, P.E. and Kulikowski, J.J., 1975. Pattern and flicker detection analyzed by subthreshold summation. *Journal of Physiology*, 249, pp.519-548.
- Kumar, R., Rattan, M., 2012. Analysis of various uality metrics for medical image processing. *International Journal of Advance Research on Computer Science and Software Engineering*, 2(11), pp.137-144.

- Legris, M., Lebart, K., Fohanno, F. and Zerr, B., 2003. Les capteurs d'imagerie en robotique sous-marine: tendances actuelles et futures. *Traitement du Signal*, 20, pp.137-164.
- McGlamery, B.L., 1979. A computer model for underwater camera systems. *Proceeding of the SPIE Ocean Optics*, 208, pp.221-231.
- Michelson, A.A., 1927. *Studies in optics*. Chicago: University of Chicago Press.
- Naim, M.J.N.M. and Isa, N.A.M., 2012. Pixel distribution shifting color correction for digital color images. *Journal of Applied Soft Computing*, 12(9), pp.2948-2962.
- Ndjahah, P., Kikuchi, H., Yukawa, M., Watanabe, H. and Muramatsu, S., 2011. An Investigation on the quality of denoised images. *International Journal of Circuit, Systems, and Signal Processing*, 5(4), pp.423-434.
- Padmavathi, G., Muthukumar, M. and Thakur, S.K., 2010. Non linear image segmentation using fuzzy c-means clustering method with thresholding for underwater images. *International Journal of Computer Sciences Issues (IJCSI)*, 7(3), pp.35-40.
- Reinagel, P. and Zador, A.M., 1999. Natural scene statistics at the center of gaze. *Network: Computation in Neural Systems*, 10, pp.1-10.
- Rizzi, A. and Gatta, C. and Marini, D., 2003. A new algorithm for unsupervised global and local color correction. *Pattern Recognition Letters*, 24(11), pp.1663-1677.
- Rizzi, A., Algeri, T., Medeghini, G. and Marini, D., 2004. A Proposal for contrast measure in digital images. *Proceeding of the Second European Conference on Color in Graphics, Imaging, and Vision (CGIV)*, Aachen, 5-8 April 2004, pp.187-192.
- Schettini, R. and Corchs, S., 2012. Underwater image processing: state of the art of restoration and image enhancement methods. *EURASIP Journal on Advances in Signal Processing*, 2010:746052.
- Schechner, Y.Y. and Karpel, N., 2004. Clear underwater vision. *Proceeding of the IEEE Conference on Computer Vision and Pattern Recognition*, Washington DC, 27 June - 2 July 2004, pp. I-536 - I-543.
- Schechner, Y.Y. and Karpel, N., 2005. Recovery of underwater visibility and structure by polarization Analysis. *IEEE Journal of Oceanic Engineering*, 30(3), pp.570-587.
- Senthilkumaran, N. and Thimmiaraja, J., 2014. Histogram equalization for image enhancement using MRI brain images. *IEEE World Congress on Computing and Communication Technologies*, Trichirappalli, 27 February - 1 March 2014, pp.80-83.
- Shamsudin, N., Ahmad, W.F.W., Baharudin, B., Rajuddin, M.K.M., 2012. Significance level of image enhancement techniques for underwater images. *International Conference on Computer & Information Sciences (ICCIS)*, Kuala Lumpur, 12-14 June 2012, pp.490-494.
- Singhai, J. and Rawat, P., 2007. Image enhancement method for underwater, ground, and satellite image using brightness preserving histogram equalization with maximum entropy. *IEEE International Conference on Computational Intelligent and Multimedia Application (ICCIMA)*, Tamil Nadu, 13-15 December 2007, pp. 507-512.
- Trucco, E. and Olmos-Antillon, A.T., 2006. Self-tuning underwater image restoration. *IEEE Journal of Oceanic Engineering*, 31(2), pp.511-519.
- Whittle, P., 1986. Increments and decrements: luminance discrimination. *Vision Research*, 26(10), pp.1677-1691.
- Wu, J., Huang, H., Qiu, Y., Wu, H., Tian, J. and Liu, J., 2005. Remote sensing image fusion based on average gradient of wavelet transform. *Proceeding of the IEEE: International Conference on Mechatronics & Automation Niagara Falls, Canada*, July 2005, pp.1817-1821.
- Wu, X. and Li, H., 2013. A simple and comprehensive model for underwater image restoration. *Proceeding of the IEEE, International Conference on Information and Automation*, Yinchuan, 26-28 August 2013, pp.699-704.
- Ye, Z., 2009. Objective assessment of nonlinear segmentation approaches to gray level underwater images. *International Journal on graphics, Vision, and Image Processing (GVIP)*, 9(2), pp.39-46.
- Yeganeh, H., Ziae, A. and Rezaei, A., 2008. A novel approach for contrast enhancement based on histogram equalization. *IEEE Proceedings of International Conference on Computer and communication Engineering*, Kuala Lumpur, 13-15 May 2008, pp.256-260.

APPENDIX A

Appendix A shows the results of 20 underwater images used to compare the output images using different methods. Images are organized based on the following methods: (a) Original image, (b) HE, (c) ICM, (d) UCM, (e) PDSCC, (f) Proposed method.

Image x		
(a)	(b)	(c)
(d)	(e)	(f)

Image 1



Image 2

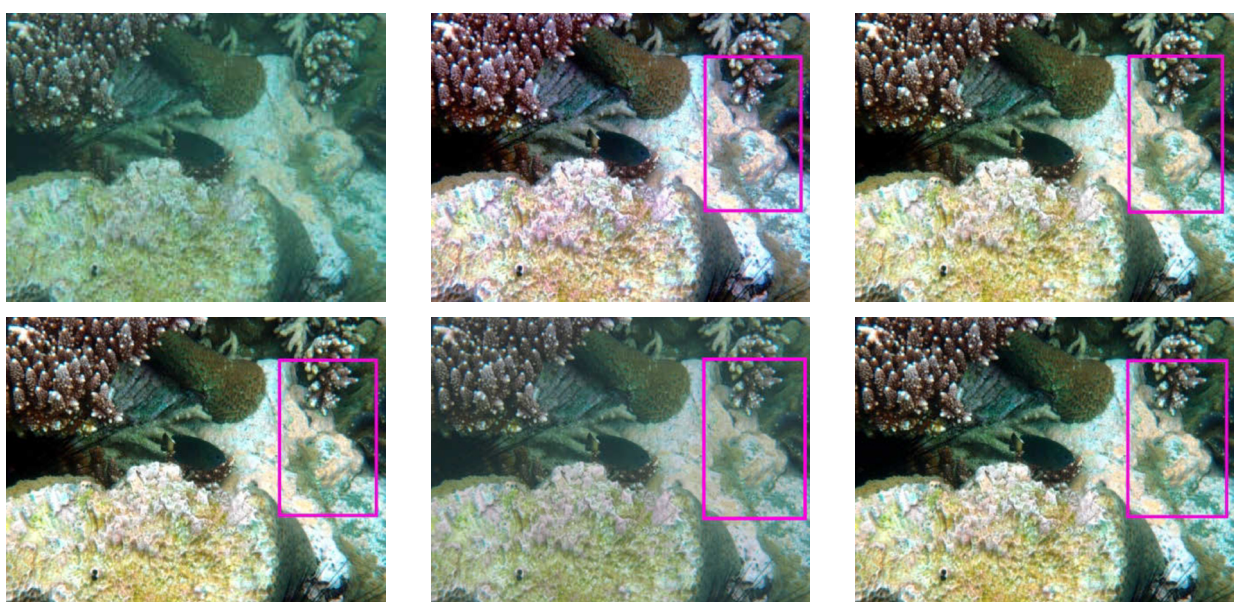


Image 3

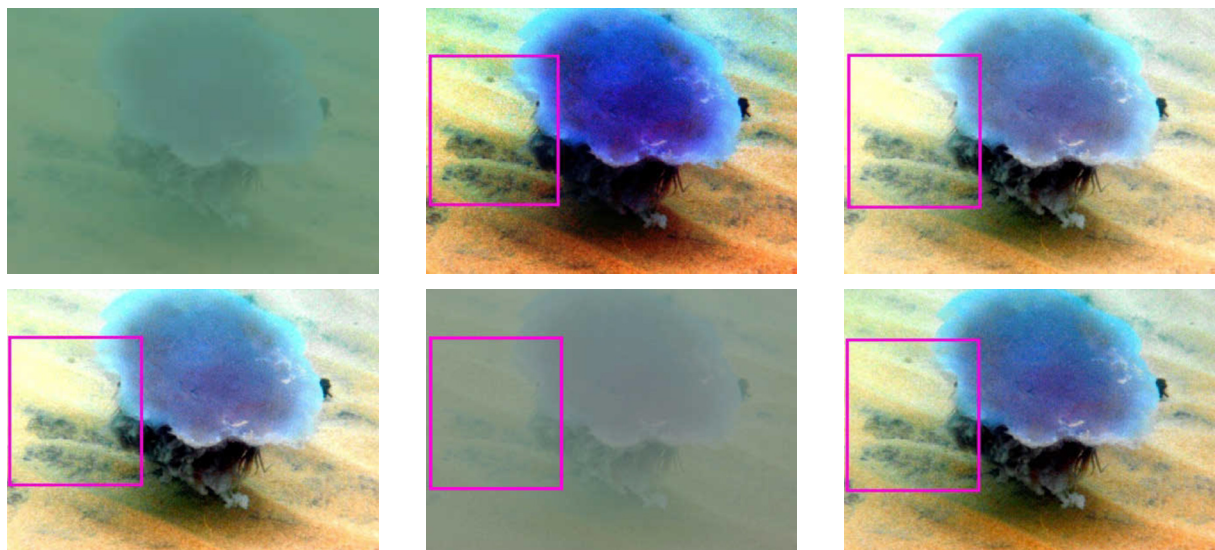


Image 4

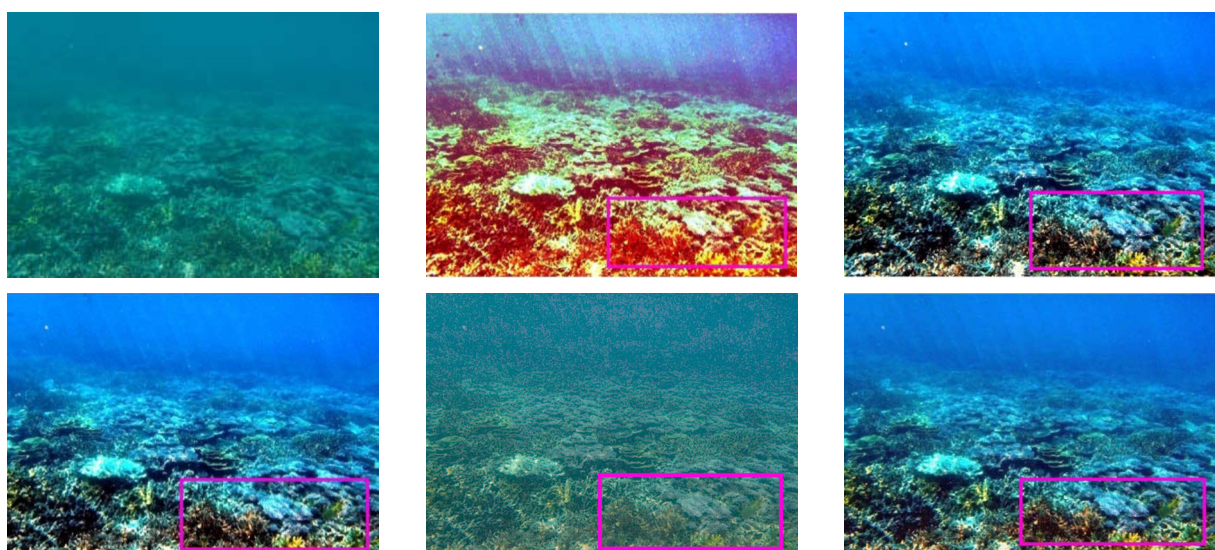


Image 5

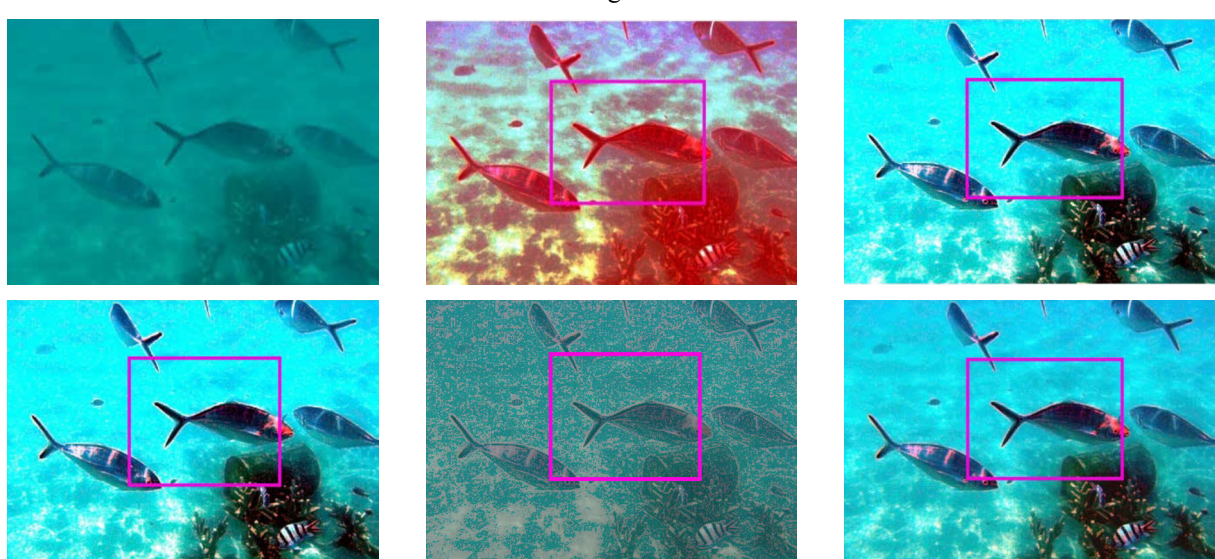


Image 6

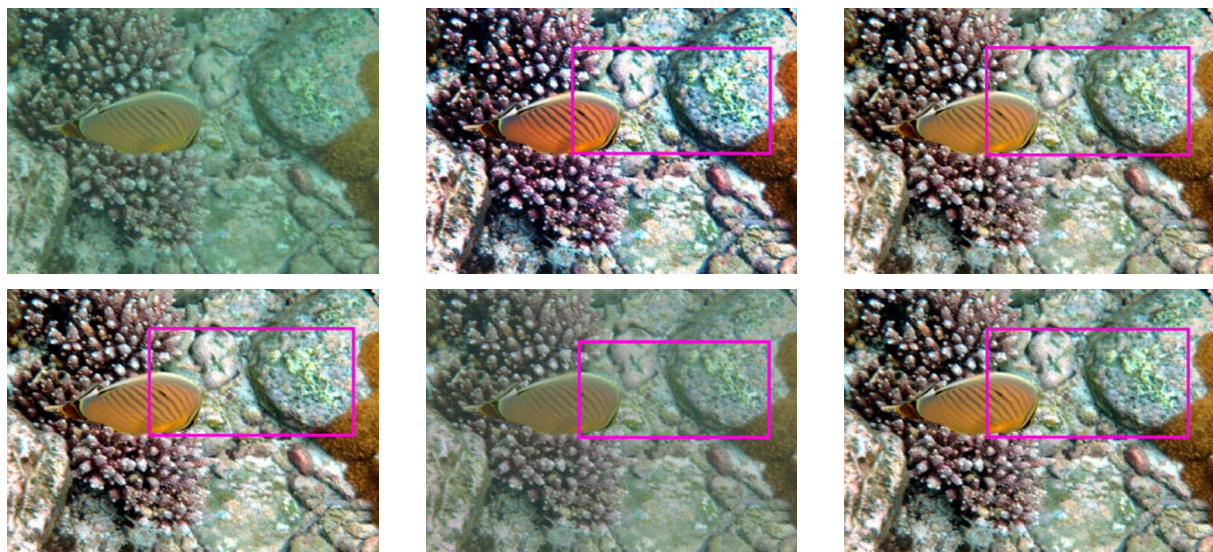


Image 7

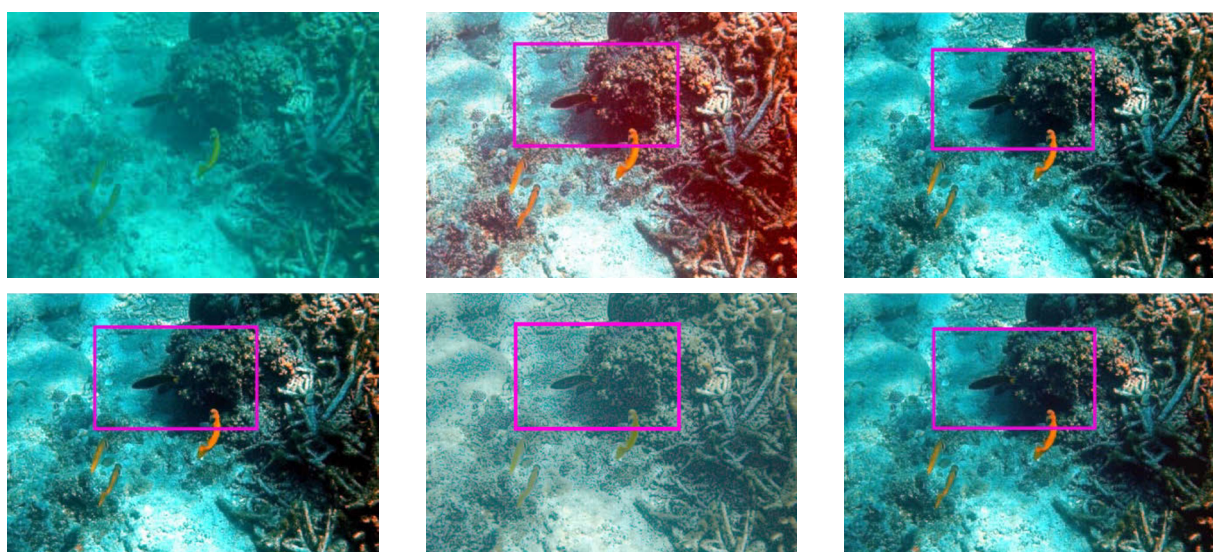


Image 8



Image 9



Image 10

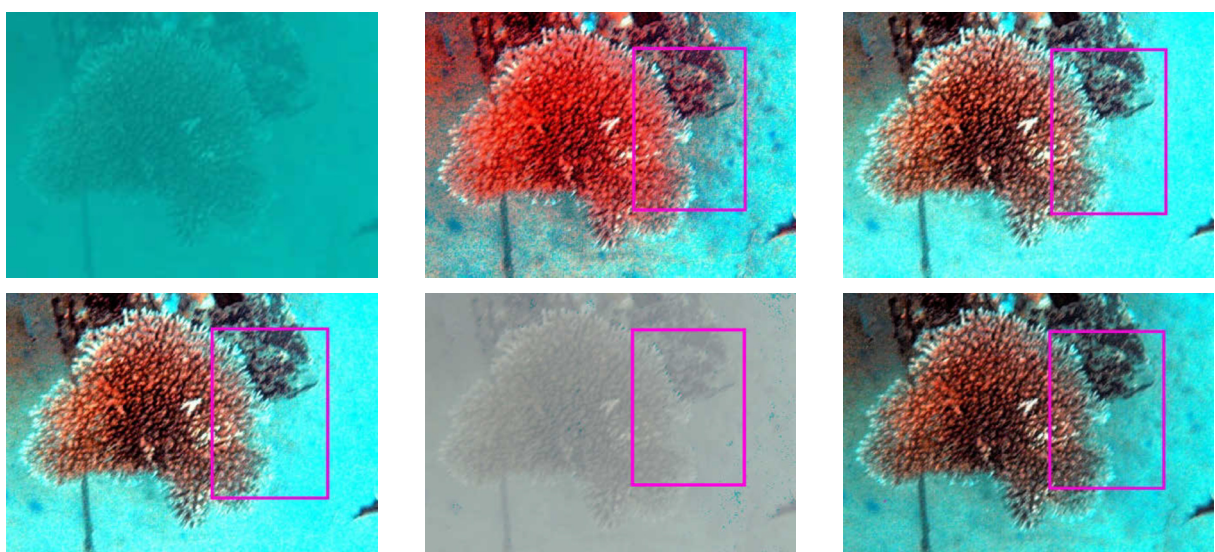


Image 11

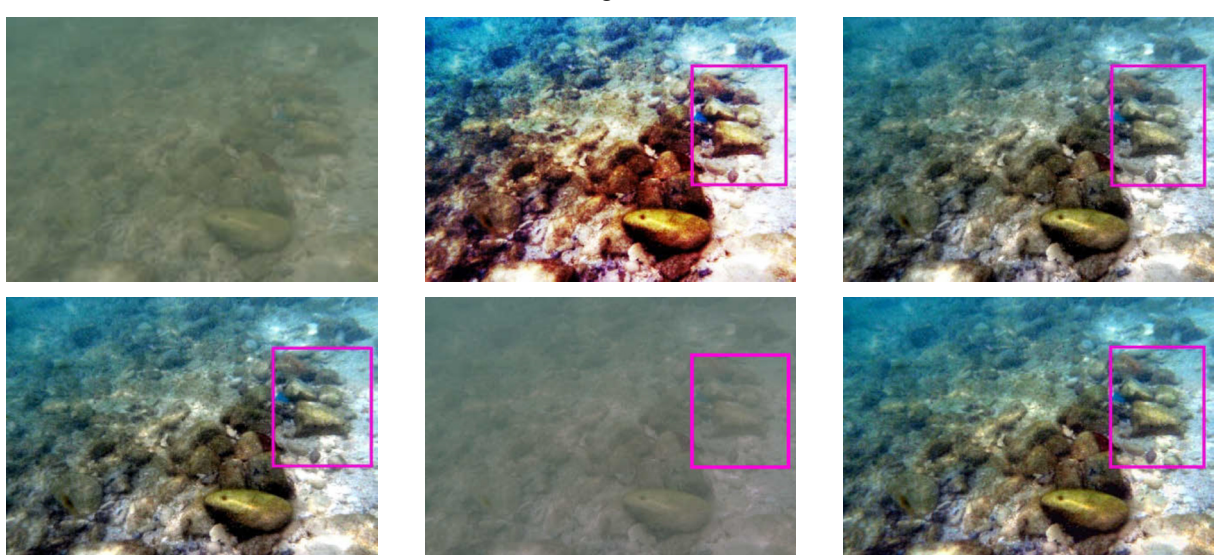


Image 12

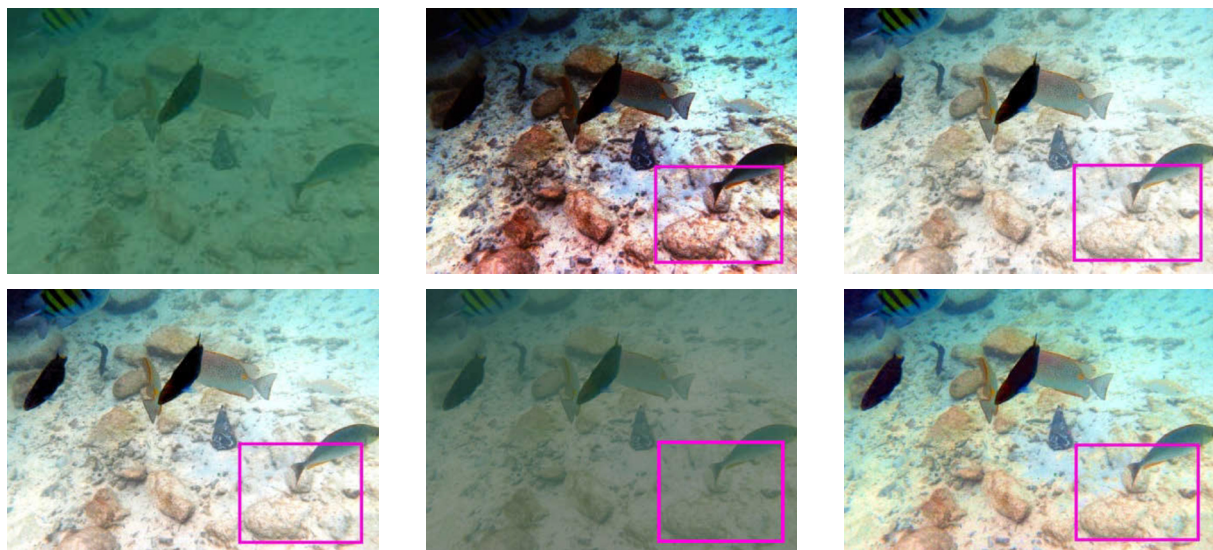


Image 13

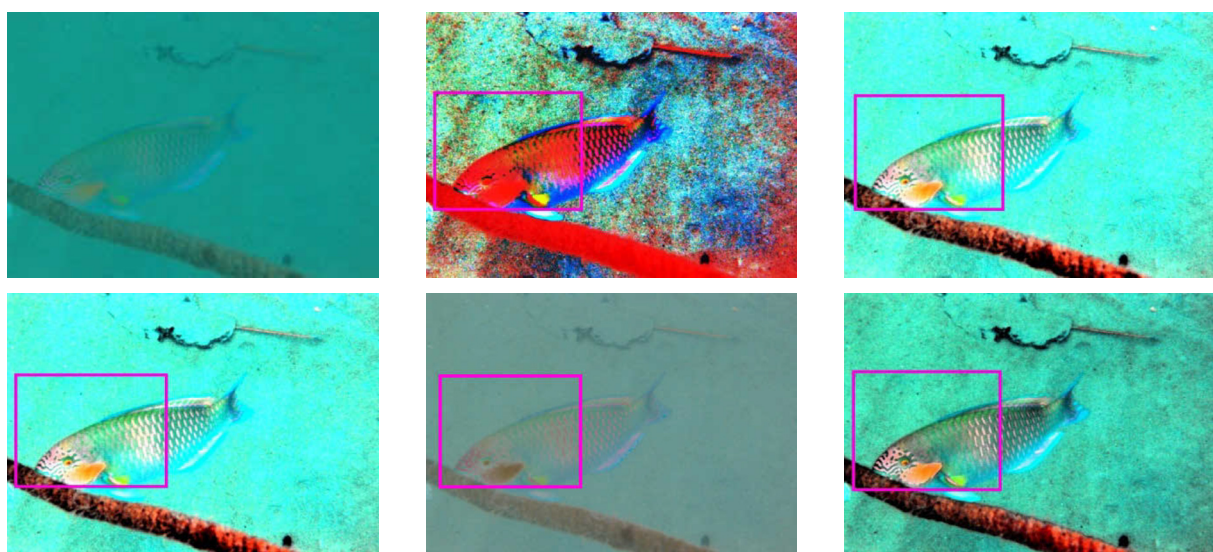


Image 14

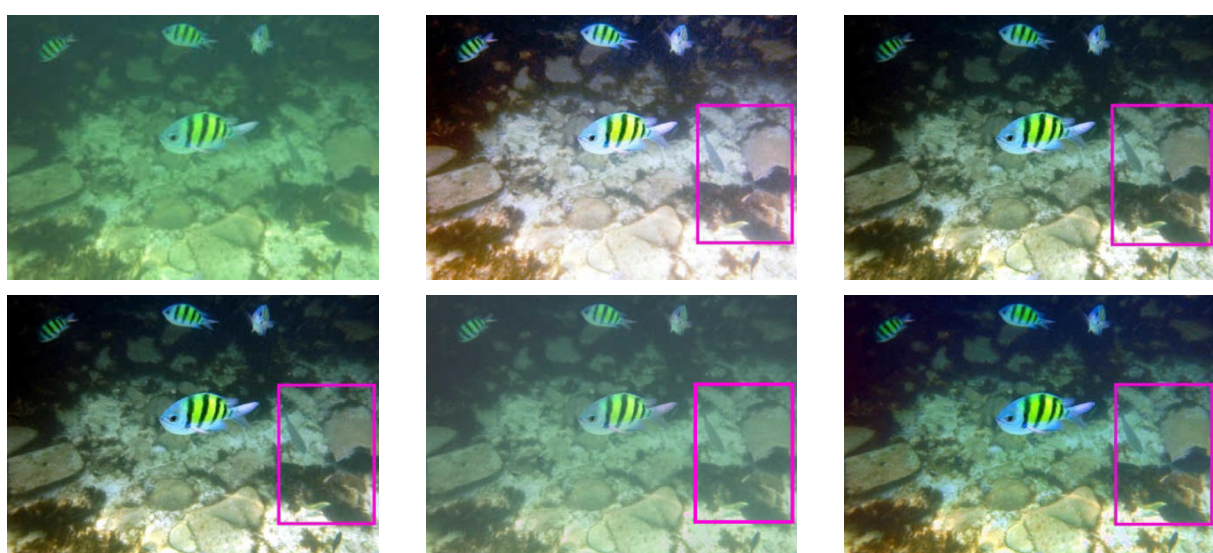


Image 15

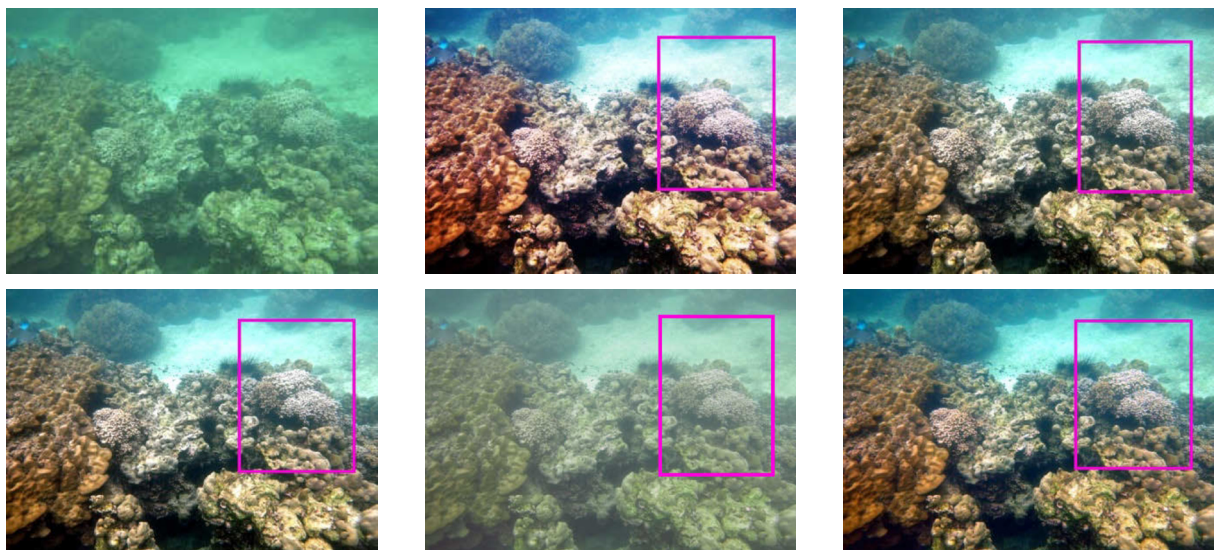


Image 16

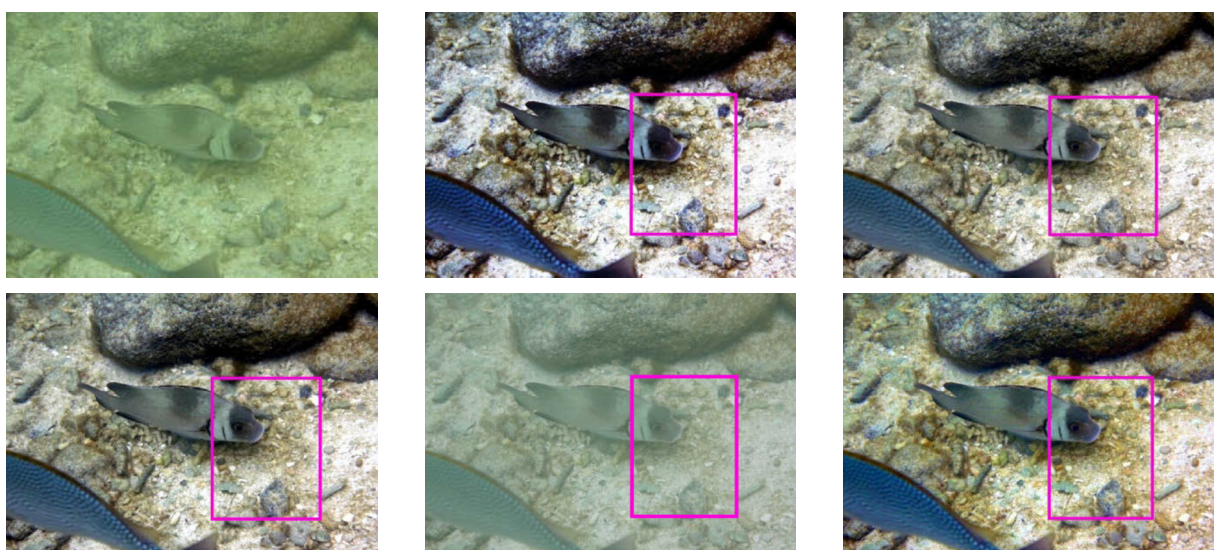


Image 17

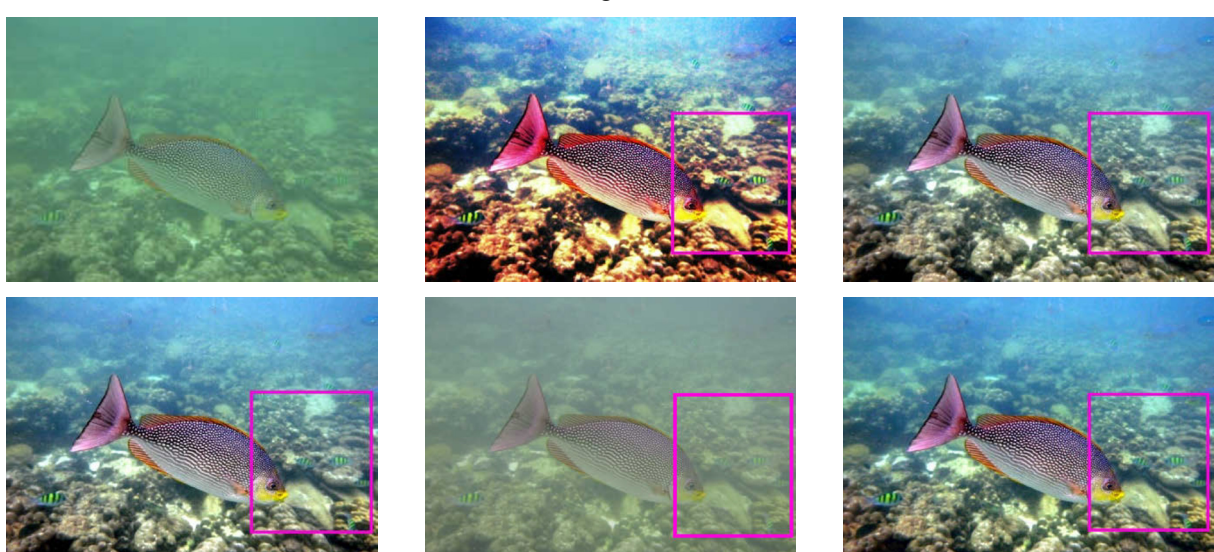


Image 18

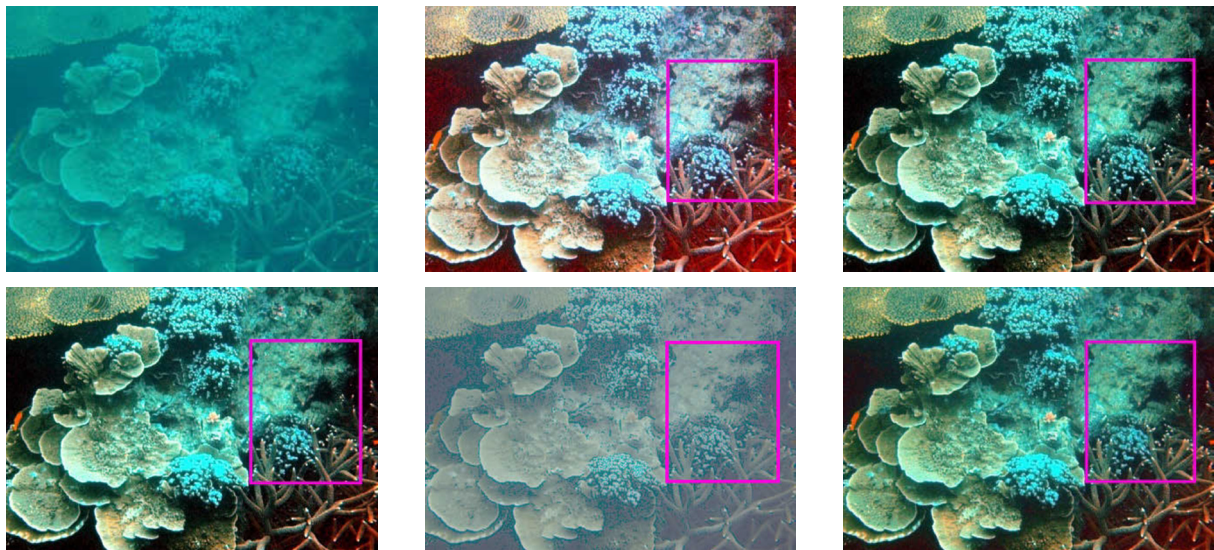


Image 19

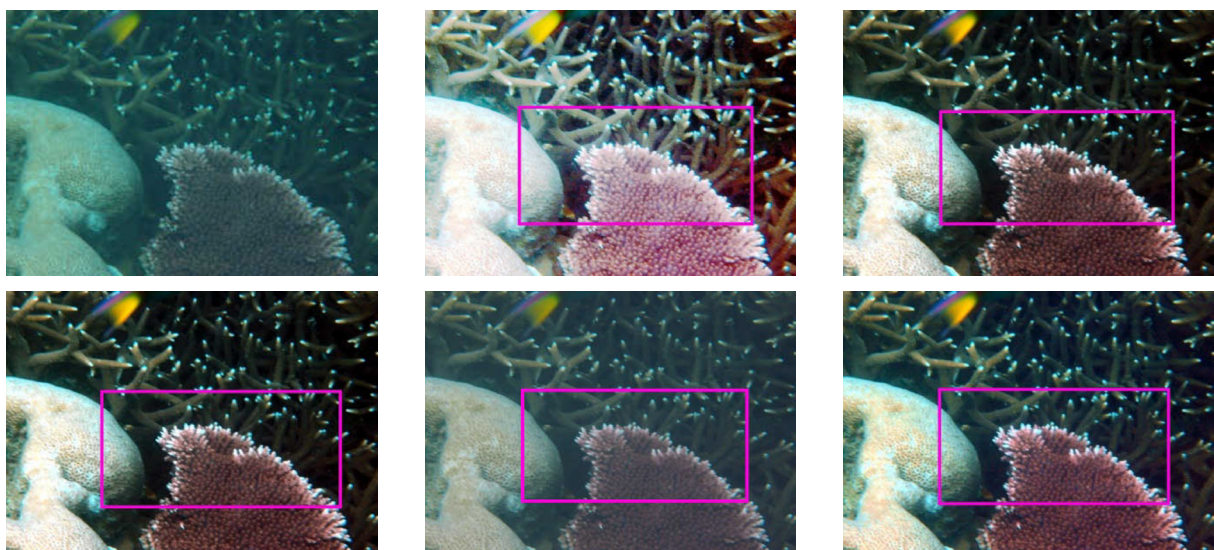


Image 20



APPENDIX B

The table in Appendix B shows the quantitative values of images in Appendix A for comparison of entropy, MSE, and PSNR values.

Image	Method parameter	HE	ICM	UCM	PDSCC	Proposed method
Image 1	Entropy	5.793	7.503	7.442	6.926	7.667
	MSE	7 874	16 074	16 090	1 777	2 736
	PSNR	9.17	6.07	6.07	15.63	13.76
Image 2	Entropy	5.990	7.897	7.905	7.484	7.949
	MSE	1 414	14 498	14 498	159	959
	PSNR	16.63	6.52	6.52	26.12	18.31
Image 3	Entropy	5.647	7.479	7.046	5.623	7.854
	MSE	4 534	15 207	15 214	202	3 541
	PSNR	11.57	6.31	6.31	25.09	12.64
Image 4	Entropy	5.415	6.901	6.697	6.31	7.429
	MSE	9 824	10 451	10 471	854	1 577
	PSNR	8.21	7.94	7.93	18.81	16.15
Image 5	Entropy	4.900	5.328	6.129	6.132	7.392
	MSE	12 635	12 430	12 455	2 171	3 019
	PSNR	7.11	7.19	7.18	14.76	13.33
Image 6	Entropy	5.986	7.852	7.865	7.158	7.872
	MSE	2 243	13 896	13 896	138	1 243
	PSNR	14.62	6.70	6.70	26.73	17.18
Image 7	Entropy	5.683	7.271	7.163	7.458	7.549
	MSE	8 049	14 630	14 638	3 472	1 749
	PSNR	9.07	6.48	6.48	12.72	15.70
Image 8	Entropy	5.957	7.674	7.631	6.553	7.757
	MSE	4 149	9 738	9 738	103	1 649
	PSNR	11.95	8.25	8.25	27.98	15.96
Image 9	Entropy	5.933	7.803	7.766	6.441	7.949
	MSE	4 288	11 217	11 224	237	2 820
	PSNR	11.81	7.63	7.63	24.39	13.63
Image 10	Entropy	5.402	6.677	7.353	5.628	7.854
	MSE	10 172	17 451	17 473	7 417	5 193
	PSNR	8.06	5.71	5.71	9.43	10.98

Image 11	Entropy	5.713	7.603	7.674	5.669	7.729
	MSE	4 487	11 865	11 865	45	1 884
	PSNR	11.61	7.39	7.39	31.64	15.38
Image 12	Entropy	5.798	7.407	6.876	6.295	7.611
	MSE	5 238	9 466	9 469	451	7 638
	PSNR	10.94	8.37	8.37	21.49	9.30
Image 13	Entropy	5.045	6.420	7.212	5.611	7.567
	MSE	8 471	13 232	13 260	2 495	2 582
	PSNR	8.85	6.91	6.91	14.16	14.01
Image 14	Entropy	5.968	7.701	7.697	7.334	7.760
	MSE	2 695	12 899	12 899	246	910
	PSNR	13.83	7.03	7.03	24.22	18.54
Image 15	Entropy	5.982	7.822	7.847	7.191	7.870
	MSE	2 775	15 726	15 729	583	1 268
	PSNR	13.70	6.16	6.16	20.48	17.10
Image 16	Entropy	5.977	7.740	7.829	6.794	7.857
	MSE	3 016	18 239	18 237	315	1 478
	PSNR	13.34	5.52	5.52	23.15	16.43
Image 17	Entropy	5.850	7.619	15 357	6.331	7.728
	MSE	4 018	15 357	15 359	310	1 457
	PSNR	12.09	6.27	6.27	23.22	16.49
Image 18	Entropy	5.666	7.561	7.387	6.635	7.740
	MSE	8 852	13 060	13 067	3 998	3 859
	PSNR	8.66	6.97	6.97	6.97	12.27
Image 19	Entropy	5.957	7.401	7.368	6.945	7.518
	MSE	5 250	7 362	7 327	263	1 282
	PSNR	10.93	9.48	9.48	23.93	17.05
Image 20	Entropy	5.887	7.565	7.728	6.139	7.806
	MSE	4 999	17 659	17 668	1 408	2 998
	PSNR	11.14	5.66	5.66	16.64	13.36

Note: The values in bold typeface represent the best results obtained in the comparison.